NTNU – Trondheim
Norwegian University of
Science and Technology

Enhanced Measurements of Large Deformations of Thermoplastics

Olve Winjum

Civil and Environmental Engineering
Submission date: Januar 2014
Supervisor: Arild Holm Clausen, KT
Co-supervisor: Marius Andersen, KT

Norwegian University of Science and Technology
Department of Structural Engineering

Department of Structural Engineering
Faculty of Engineering Science and Technology
NTNU- Norwegian University of Science and Technology

ACCESSIBILITY

OPEN

MASTER THESIS 2014

SUBJECT AREA:	DATE:	NO. OF PAGES:
POLYMER ENGINEERING	13 JANUARY 2014	71 + 22

TITLE:

Enhanced measurements of large deformations of thermoplastics

Forbedret måling av store deformasjoner av plastmaterialer

BY:

Olve Winjum

SUMMARY:

The purpose of this study is to evaluate a numerical material model for thermoplastics developed at SIMLab, NTNU. Several experimental tests, using both HDPE and PVC, were conducted in order to have a basis for calibrating the material model. The focus of this thesis has been on optimizing the methods for retrieving the results of the experimental tests and numerical simulations.

3D digital image correlation (DIC) was used to obtain the strains from the experimental tests. This proved very successful for the tension tests, but did not work well for longitudinal strains of the compression tests, which had to be calculated from the displacement. The 3D DIC analysis also allows for test specimens with circular cross sections to be used. These specimens proved to get better results than the quadratic specimens used in previous studies.

Obtaining the strains from the numerical simulations was done by two different methods. One method was getting the strains directly from all the elements in one cross section; the other was calculating the strains from the displacement of the nodes on the surface of the specimen. This last method is equivalent to the DIC analysis, and resulted in a better match between the experimental and simulation results of the tension tests.

The numerical model was largely able to reproduce the results of the experimental tests. The biggest problem seems to stem from the simulations having a higher strain rate than the experimental tests.

RESPONSIBLE TEACHER: Professor Arild Holm Clausen

SUPERVISOR(S): Arild Holm Clausen, Marius Endre Andersen

CARRIED OUT AT: Simlab, NTNU

NORGES TEKNISK-NATURVITENSKAPELIGE UNIVERSITET
INSTITUTT FOR KONSTRUKSJONSTEKNIKK

MASTER THESIS 2013

Olve Winjum

Pressure sensitivity of thermoplastics

(Trykkavhengighet av plastmaterialer)

As a part of the development of the finite element method, significant effort has been devoted to propose new material models which are able to represent the material behaviour at different conditions. Relevant parameters involve strain level, strain rate, temperature, and the material at hand may also exhibit anisotropy, viscoelasticity etc. Unlike metals, a particular feature with most polymer materials is that they exhibit pressure sensitivity, i.e. the yield stress is larger in compression than in tension. In a material model, the yield stress is represented with a yield criterion. Moreover, the subsequent plastic deformation after onset of yielding is also dependent on the pressure level in polymers. This is mathematically described with a flow potential. The pressure sensitivity is also linked to possible change of volume in the material during plastic deformation.

The intention with this master thesis is to explore different aspects related to pressure sensitivity from both an experimental and a modeling point of view. Applying a material model developed at SIMLab, a function proposed by Raghava and co-workers is employed for both the yield criterion and plastic potential. Moreover, the entropy-elastic part of the total deformation is also significant for polymers. The candidate shall evaluate how the contributions from elasticity, yield function and plastic potential in the model are able to represent observed physical behaviour. Special attention will be paid to tests in compression. Careful experimental tests are required for the addressed investigation, calling for precision measurements of the strains at large deformations.

Possible keywords for activities in this master thesis research work may include:

- Literature: Polymers in general, material models, pressure sensitivity
- Experimental tests: Material tests. Presentation and interpretation of test results
- Numerical modelling: Simulation of experimental tests. Evaluation of the model

The candidate may agree with the supervisors to pay particular attention to specific parts of the investigation, or include other aspects than those already mentioned.

The thesis is to be organized as a research report, recognising the guidelines provided by Department of Structural Engineering.

Supervisors: Arild Holm Clausen and Marius Andersen

The report is to be handed in not later than 15 January 2014.

NTNU, 21 August 2013

Arild Holm Clausen

Abstract

The purpose of this study is to evaluate a numerical material model for thermoplastics developed at SIMLab, NTNU. Several experimental tests, using both HDPE and PVC, were conducted in order to have a basis for calibrating the material model. The focus of this thesis has been on optimizing the methods for retrieving the results of the experimental tests and numerical simulations.

3D digital image correlation (DIC) was used to obtain the strains from the experimental tests. This proved very successful for the tension tests, but did not work well for longitudinal strains of the compression tests, which had to be calculated from the displacement. The 3D DIC analysis also allows for test specimens with circular cross sections to be used. These specimens proved to get better results than the quadratic specimens used in previous studies.

Obtaining the strains from the numerical simulations was done by two different methods. One method was getting the strains directly from all the elements in one cross section; the other was calculating the strains from the displacement of the nodes on the surface of the specimen. This last method is equivalent to the DIC analysis, and resulted in a better match between the experimental and simulation results of the tension tests.

The numerical model was largely able to reproduce the results of the experimental tests. The biggest problem seems to stem from the simulations having a higher strain rate than the experimental tests.

Sammendrag

Hensikten med denne studien er å evaluere en numerisk materialmodell for plastmaterialer utviklet ved SIMLab, NTNU. Flere eksperimentelle tester, med både HDPE og PVC, ble utført som en basis for kalibrering av materialmodellen. Fokus for denne oppgaven har vært på optimaliseringen av metoder for å hente ut resultatene fra eksperimentelle tester og numeriske simuleringer.

3D digital bilde korrelasjon (DIC) ble anvendt for å hente ut tøyningene fra de eksperimentelle testene. Dette viste seg å være svært vellykket for strekktestene, men fungerte ikke så bra for lengdetøyningene i kompresjonstestene, som måtte beregnes ut fra forskyving. 3D DIC analyse gjør det også mulig å benytte prøvestykker med sirkulært tverrsnitt. Disse prøvestykkene viste seg å gi bedre resultater enn de kvadratiske prøvestykkene brukt i tidligere studier.

Uthenting av tøyninger fra de numeriske simuleringene ble gjort med to forskjellige metoder. En metode var å få tøyningene direkte fra alle elementene i et tverrsnitt; den andre var å beregne tøyningene fra forskyvningen av nodene på overflaten av prøven. Denne siste metoden er ekvivalent med DIC analyse, og ga bedre samsvar mellom resultatene fra de eksperimentelle og simulerte strekktestene.

Den numeriske modellen var i stor grad i stand til å reprodusere resultatene fra de eksperimentelle testene. Det største problemet synes å stamme fra at simuleringene har en høyere tøyningshastighet enn de eksperimentelle testene.

Acknowledgements

This master thesis was written at Structural Impact Laboratory at Norwegian University of Science and Technology, NTNU, as part of a larger study on a numerical material model for polymers.

I would like to thank my supervisor Professor Arild Holm Clausen for his guidance and support in the process of writing this thesis. Also, Ph.D. candidate Marius Andersen deserves thanks, his tutoring throughout the work has been vital.

A special thanks also goes to Trond Auestad for carrying out the experimental tests, and to Egil Fagerholt for calibrating the camera setup for the tests and for giving a great introduction into digital image correlation.

Trondheim, 13th January, 2014

Olve Winjum

Contents

Chapter 1

Introduction

Due to their relatively low strength, polymers have historically been used mostly for packaging, and not as a structural material. More recently, however, polymers have also come into use for structural purposes. The low weight of polymers have made them attractive materials for many industries. Using additives, the material properties of polymers can also be changed in order to meet specific needs.

In order to study the material behavior of polymers, NTNU's Structural Impact Laboratory (SIMLab) has developed a numerical material model for polymers in the finite element program LS-DYNA. This thesis will use experimental results to calibrate the parameters in the material model, and try to reproduce the experimental tests using numerical simulations. Experimental tests using two different materials, high-density polyethylene (HDPE) and polyvinyl chloride (PVC), have been carried out. The study will focus on determining the most accurate ways to evaluate the results of both experiments and simulations.

The report will start with theory on polymers in general, the material model used in this study and the method of determining the strains of the experimental tests. Then, the testing procedure and the results from the tests are presented. A description of how the material model was calibrated from the experimental results is then given. Next, the numerical simulations are presented. And lastly, a conclusion and suggestions to further work is given.

Chapter 2

Theory

This chapter will present the theory behind the experiments and analyses performed in this study. First is a description of polymers, especially focusing on the two materials tested in this study. Then, an explanation is given of the material model used for the numerical simulations in Chapter 6. Lastly, a presentation of digital image correlation will be given; this is a method used for obtaining strains from the experimental tests.

2.1 Polymers

This section will give an introduction to polymers in general, with extra details about high-density polyethylene (HDPE) and polyvinyl chloride (PVC), the two materials used in this study. The information here is largely based on two books, where Ram[1] explains the polymerization process, and Rösler et al.[2] describes the material behavior.

Polymers are large macromolecules that consist of long chains of identical parts called mers. Mers are made from monomers, which are molecules that are able to go through the process of polymerization. To do this, the molecule must have either a covalent double bond or two functional groups.

Monomers with two functional groups, e.g. one hydroxyl (OH) group and one carboxyl (COOH) group, go through a process called stepwise polymerization. This process is characterized by condensation reactions between the molecules. The functional groups react and are bound together, also creating H_2O as a byproduct. At the start of the stepwise polymerization process, many small chains of two to four mers are created. Since there are always functional groups at both ends of every chain, these smaller chains can connect to make longer chains.

The monomers with covalent double bonds are created by a different process, called chain polymerization, characterized by addition reactions. These reactions are initiated by adding a chemical with a free radical to the monomers. This chemical can react with a monomer by breaking the double bond, and at the same time create a free radical on the monomer. This can in turn attach itself to another monomer by breaking its double bond. Thus, the monomers are added to the chain one by one. The addition reactions do not create any byproducts.

Ethylene is the simplest form of a monomer with a covalent double bond. It consists of two carbon atoms with a double bond between them, and two hydrogen atoms bound to each carbon atom. Ethylene is the basis of a whole group of monomers, called vinyls. All vinyls have the same molecular structure as ethylene, except that one of the hydrogen atoms is substituted by either another atom or a whole group, e.g. CH_3 which results in propylene.

Polymer chains can consist up to several thousand mers. The average chain length is a measure of the degree of polymerization. Polymers can be divided into three main groups, thermoplastics, elastomers and thermosets. Elastomers and thermosets also have covalent bonds between the chains, which inhibits almost all relative movement of the chains. This gives these polymers a rubbery effect, and no plastic deformation is possible. The two materials tested in this study are both thermoplastics, and have therefore no cross-bonds between the chains.

A property that is unique to thermoplastics, due to the lack of cross-bonds, is crystallinity. This means that the polymer chains in some areas of the material fold up neatly and get more tightly packed here than in other parts. It is impossible to achieve full crystallinity, and there will always be some areas with an amorphous structure. Figure 2.1 illustrates this, with two crystalline areas and an amorphous part in between. A high degree of crystallinity increases both the stiffness and the yield strength of the material.

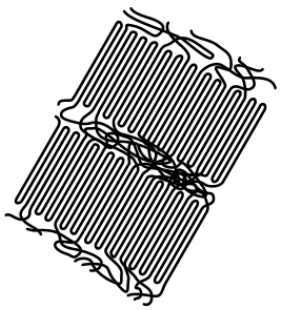

Figure 2.1: Crystalline polymer[2]

Even though thermoplastics do not form cross-bonds between the chains, they can have shorter branches going off the main stem of the molecule. More branches means less crystallinity, as the chains are not able to form the regular structure of crystalline materials. This results in a more amorphous structure, which gives the material lower stiffness and strength, but higher ductility.

There are two sources of elastic resistance in polymers. At small deformations, the van der Waals or hydrogen bonds between the chains accounts for most of the resistance.

At larger deformations, straightening of the molecule chains causes an increased resistance. During elastic deformation the points of entanglement between the chains remains the same, as illustrated in Figure 2.2. Since the chains have not moved in relation to each other, this deformation is completely reversible.

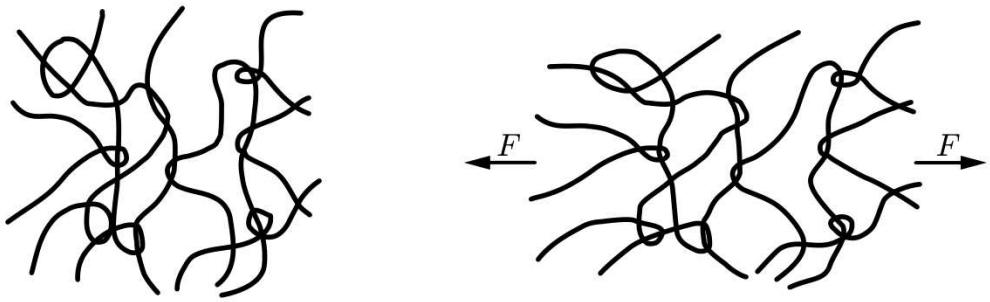

Figure 2.2: Elastic deformation of a polymer[2]

The plastic deformation starts when the forces are so large that the polymer chains start sliding relative to each other. Figure 2.3 shows a polymer chain inside a larger polymer structure. Due to the dense structure around the chain, the angles of the atoms in the molecule have to go through a reconfiguration in order to move in relation to the other chains. As seen in Figure 2.4, a rotation of the polymer chains demands an energy potential to be passed in order to reach a new stable configuration. This type of deformation is plastic, and will not be reverted when the material is unloaded.

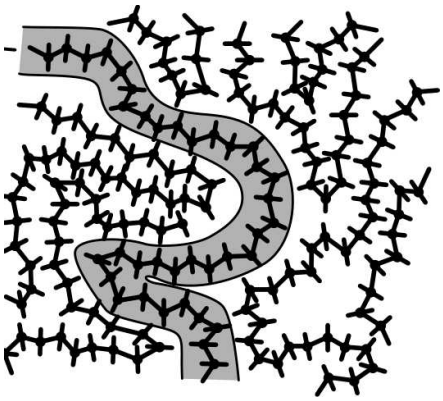

Figure 2.3: A polymer chain[2]

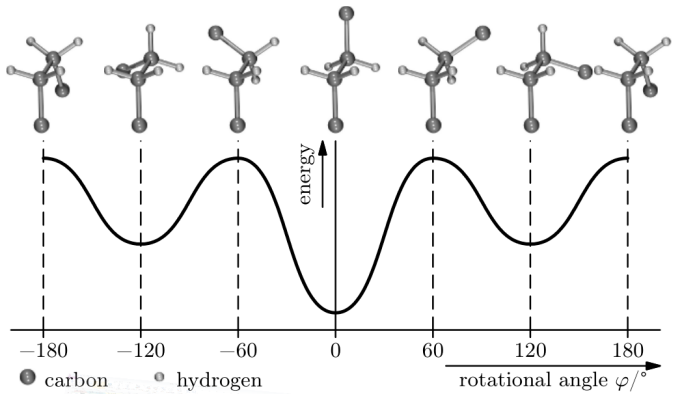

Figure 2.4: Potential energy of different chain configurations[2]

If a polymer is subjected to tensile stress, as seen in Figure 2.5, a region with an initial weakness will reach yielding first. The polymer chains in this region will start to straighten out and glide past each other. The material will then start necking, concentrating the stress in this region. Further yielding is also helped by a rise in temperature due to friction between the chains.

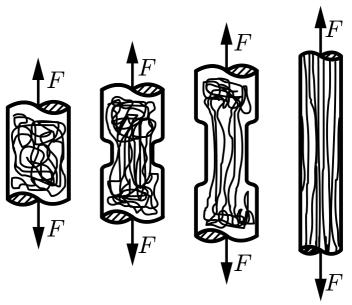

Figure 2.5: Propagation of neck[2]

When the chains at the neck are straightened out in the tensile direction, the stiffness in this region increases. The capacity of the covalent bonds in the chains is much higher than the intermolecular resistance. Further straightening the chains at both ends of the neck therefore requires less energy than breaking the already straight parts of the chains. This causes the neck to propagate along the material until all the polymer chains are stretched in the tensile direction.

2.1.1 High-density polyethylene

High-density polyethylene (HDPE) is made through polymerization of ethylene. Figure 2.6 shows the molecular structure of these compounds.

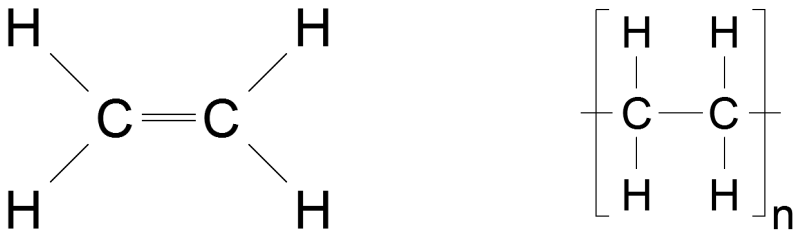

(a) Ethylene (b) Polyethylene

Figure 2.6: Molecular structures of ethylene and polyethylene

HDPE consists of long chains with very few branches. This allows for a very high degree of crystallininty, up to 80-90%. The chains are packed very tightly, hence the high density. The high degree of crystallinity makes HDPE stiffer and stronger than other types of polyethylene with more branches on the chains, but the ductility is somewhat reduced.

2.1.2 Polyvinyl chloride

Polyvinyl chloride (PVC) is made through polymerization of vinyl chloride. This is a vinyl where one hydrogen atom of ethylene is substituted by a chloride atom, as seen

in Figure 2.7.

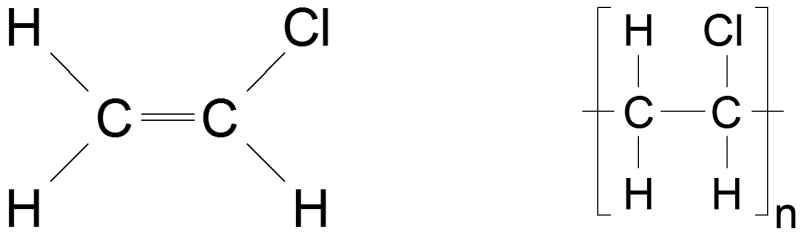

(a) Vinyl chloride

(b) Polyvinyl chloride

Figure 2.7: Molecular structures of vinyl chloride and polyvinyl chloride

The substitution of hydrogen for chloride causes the polymer chains to have a much higher polarity. This means that the forces between the chains become stronger and give the material a higher stiffness and yield strength.

2.2 Material model

The material model used for the numerical simulations in Chapter 6 was developed by Polanco-Loria et al.[3] at SIMLab. It is described by the rheological model in Figure 2.8. This section will describe the equations and principles behind the model; it is based on the description of the model by Polanco-Loria et al. and previous work done by Hovden[4].

The resistance is split into two parts; part A describes the intermolecular resistance, while part B describes the resistance due to orientation of the polymer network. Part A of the rheological model consists of an elastic spring describing the initial stiffness, a friction element describing yielding and plastic flow, and a dashpot describing the rate dependence. Part B consists of a spring that has an evolving resistance due to molecular orientation.

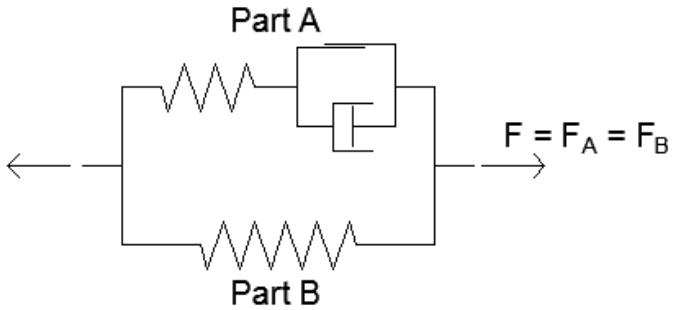

Figure 2.8: Rheological model

From the rheological model, it can be seen that the deformation gradient is the same for both parts:

$$\boldsymbol{F} = \boldsymbol{F}_A = \boldsymbol{F}_B \tag{2.1}$$

This means that the volume change, given as the determinant of the deformation gradient, is also the same for both parts:

$$J_A = J_B = J = \det \boldsymbol{F} \tag{2.2}$$

The Cauchy stress tensor is obtained by summing the contributions from the two parts:

$$\boldsymbol{\sigma} = \boldsymbol{\sigma}_A + \boldsymbol{\sigma}_B \tag{2.3}$$

The stress-strain curve for each part, and the combined curve is shown in Figure 2.9. The dashed lines illustrates an extra effect of hardening or softening in the material that can occur after yielding.

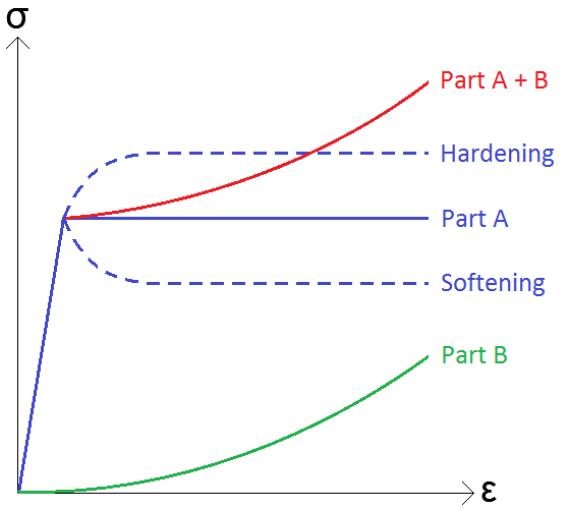

Figure 2.9: Stress-strain curve of each part

2.2.1 Part A: Intermolecular resistance

The spring in part A, is defined by two elastic parameters λ_0 and μ_0. These can be determined starting with the elastic constitutive law in terms of the Kirchhoff stress $\boldsymbol{\tau}_A$, defined by

$$\boldsymbol{\tau}_A = \lambda_0 \ln J_A^e \boldsymbol{I} + \mu_0 \left(\boldsymbol{B}_A^e - \boldsymbol{I}\right) \tag{2.4}$$

which relates to the Cauchy stress according to Equation (2.5)

$$\boldsymbol{\tau}_A = J_A^e \boldsymbol{\sigma}_A \tag{2.5}$$

Combining Equations (2.4) and (2.5) yields

$$\boldsymbol{\sigma}_A = \frac{\lambda_0}{J_A^e} \ln J_A^e \boldsymbol{I} + \frac{\mu_0}{J_A^e} \left(\boldsymbol{B}_A^e - \boldsymbol{I} \right) \tag{2.6}$$

where $\boldsymbol{I}$ is the second-order unit tensor, and $\boldsymbol{B}_A^e = \boldsymbol{F}_A^e \left(\boldsymbol{F}_A^e \right)^T$ is the left Cauchy-Green deformation tensor. λ_0 and μ_0 are the Lamé constants, and can be substituted by Young's modulus E and Poisson's ratio ν through Equations (2.7) and (2.8) [5]

$$\lambda_0 = \frac{\nu E}{(1+\nu)(1-2\nu)} \tag{2.7}$$

$$\mu_0 = \frac{E}{2(1+\nu)} \tag{2.8}$$

The friction element in part A, which controls yielding in the material, is governed by Equation (2.9)

$$f_A = \bar{\sigma}_A - \sigma_T - R\left(\varepsilon_A^p\right) = 0 \tag{2.9}$$

Each term in this expression will be explained in the following text. The yield criterion used is one proposed by Raghava[6]; this criterion has been shown to be accurate for polymers in uniaxial and biaxial tension, and in bending[4][7]. The Raghava yield function is given as

$$(\sigma_1 - \sigma_2)^2 + (\sigma_2 - \sigma_3)^2 + (\sigma_3 - \sigma_1)^2 + 2\left(|\sigma_C| - |\sigma_T|\right)(\sigma_1 + \sigma_2 + \sigma_3) = 2\,|\sigma_C \sigma_T| \tag{2.10}$$

where σ_1, σ_2 and σ_3 are the three principal stresses, and σ_C and σ_T are the yield stresses in compression and tension respectively.

The first principal invariant of the total stress I_1, and the second principal invariant of the deviatoric stress J_2 are defined by Equations (2.11) and (2.12) [5]

$$I_1 = \sigma_1 + \sigma_2 + \sigma_3 \tag{2.11}$$

$$J_2 = \frac{1}{6}\left[(\sigma_1 - \sigma_2)^2 + (\sigma_2 - \sigma_3)^2 + (\sigma_3 - \sigma_1)^2\right] \tag{2.12}$$

Introducing these into Equation (2.10), it can be rewritten as

$$3J_2 + \left(|\sigma_C| - |\sigma_T|\right) I_1 = |\sigma_C \sigma_T| \tag{2.13}$$

A parameter α is defined as the ratio between the yield stresses in compression and tension

$$\alpha = \left| \frac{\sigma_C}{\sigma_T} \right| \geq 1 \tag{2.14}$$

Equation (2.13) can now be further simplified to

$$\alpha \sigma_T^2 - (\alpha - 1) I_1 \sigma_T - 3J_2 = 0 \tag{2.15}$$

The yield criterion can then be written on the form

$$f_A\left(I_1, J_2\right) = \alpha\sigma_T^2 - \left(\alpha - 1\right) I_1\sigma_T - 3J_2 = \bar{\sigma}_A - \sigma_T = 0 \tag{2.16}$$

where $\bar{\sigma}_A$ is the equivalent stress defined by

$$\bar{\sigma}_A = \frac{\left(\alpha - 1\right) I_{1A} + \sqrt{\left(\alpha - 1\right)^2 I_{1A}^2 + 12\alpha J_{2A}}}{2\alpha} \tag{2.17}$$

The yielding follows a non-associated flow rule with a plastic potential g_A which has an expression similar to the equivalent stress in Equation (2.17). It is given as

$$g_A = \frac{\left(\beta - 1\right) I_{1A} + \sqrt{\left(\beta - 1\right)^2 I_{1A}^2 + 12\beta J_{2A}}}{2\beta} \tag{2.18}$$

where the parameter $\beta \geq 1$ controls the volumetric plastic strain.

An alteration to the Raghava yield criterion is introduced by adding an option of hardening or softening after yielding[4]. This behavior is governed by two parameters, the saturation stress σ_S and a ramping parameter H which controls the material behavior between σ_T and σ_S. These parameters are implemented into the model by the expression

$$R\left(\varepsilon_A^p\right) = \left(\sigma_S - \sigma_T\right)\left[1 - \exp\left(-H\varepsilon_A^p\right)\right] \tag{2.19}$$

where ε_A^p is the plastic strain in part A. It can be seen from Equations (2.9) and (2.19) that a higher σ_S than σ_T means there is hardening in the material after yielding, while a σ_S lower than σ_T means the material softens after yielding. This is illustrated in Figure 2.10. The parameter H is here shown determining the radius of the curve between σ_T and σ_S.

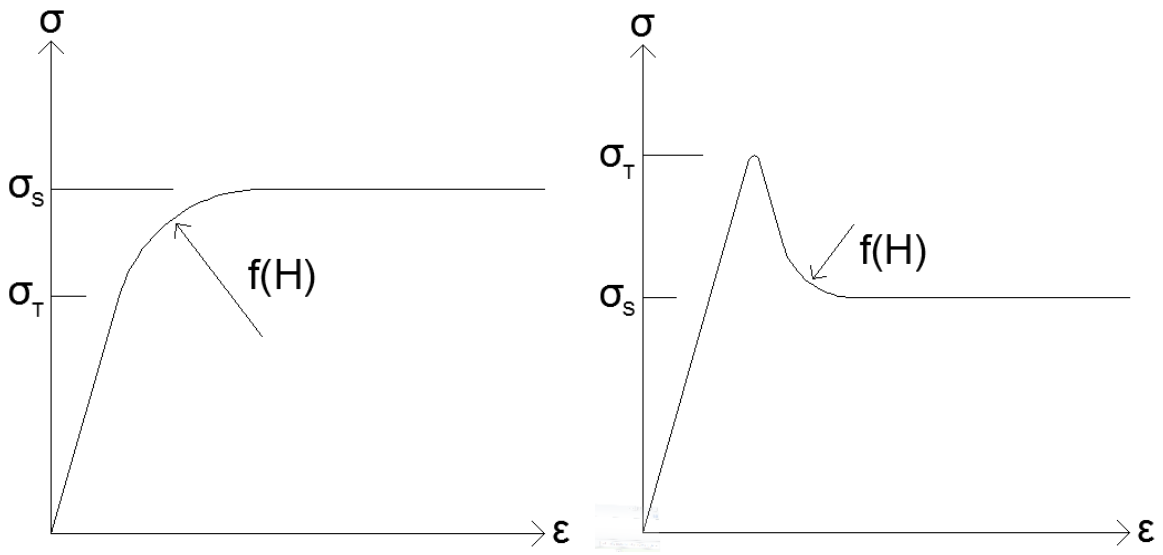

(a) Hardening (b) Softening

Figure 2.10: Illustration of the hardening/softening parameters σ_S and H

The dashpot in part A controls the strain rate dependence of the material. The plastic strain rate is found from Equation (2.20)

$$\dot{\bar{\varepsilon}}_A^p = \begin{cases} 0 & \text{if } f_A \leq 0 \\ \dot{\varepsilon}_{0A} \left\{ \exp\left[\frac{1}{C} \left(\frac{\bar{\sigma}_A}{\sigma_T} - 1 \right) \right] - 1 \right\} & \text{if } f_A > 0 \end{cases} \tag{2.20}$$

where f_A is the yield criterion from Equation (2.9). The two parameters that has to be determined are a reference strain rate $\dot{\varepsilon}_{0A}$ and a temperature-dependent strain rate sensitivity parameter C. These can easily be obtained from experimental tests with varying strain rates.

2.2.2 Part B: Network resistance

The spring in part B represents the resistance of the molecular network as the molecule chains are stretched out in the tensile direction. The elastic constitutive law in terms of the Kirchhoff stress $\boldsymbol{\tau}_B$ is defined as

$$\boldsymbol{\tau}_B = \frac{C_R}{3} \frac{\bar{\lambda}_L}{\bar{\lambda}} \mathscr{L}^{-1} \left(\frac{\bar{\lambda}}{\bar{\lambda}_L} \right) \left(\boldsymbol{B}_B^* - \bar{\lambda}^2 \boldsymbol{I} \right) + \kappa \left(\ln J_B \right) \boldsymbol{I} \tag{2.21}$$

The parameter κ is a bulk modulus mostly used when simulating materials like rubber, it will therefore be set equal to zero and not used any further in this thesis. Since the relation between Kirchhoff and Cauchy stress given in Equation (2.5) also can be

used for part B, the Cauchy stress is given as

$$\boldsymbol{\sigma}_B = \frac{C_R}{3J_B}\frac{\bar{\lambda}_L}{\bar{\lambda}}\mathscr{L}^{-1}\left(\frac{\bar{\lambda}}{\bar{\lambda}_L}\right)\left(\boldsymbol{B}_B^* - \bar{\lambda}^2\boldsymbol{I}\right) \tag{2.22}$$

$\boldsymbol{B}_B^* = \boldsymbol{F}_B^*(\boldsymbol{F}_B^*)^T$ is here the distortional left Cauchy-Green deformation tensor, and $\boldsymbol{F}_B^* = J_B^{-1/3}\boldsymbol{F}_B$ is the distortional part of $\boldsymbol{F}_B$. J_B is the Jacobian from Equation (2.2), and $\mathscr{L}^{-1}$ is the inverse function of the Langevin function defined as

$$\mathscr{L}(x) = \coth x - \frac{1}{x} \tag{2.23}$$

$\bar{\lambda}$ is the distortional stretch and can be determined by

$$\bar{\lambda} = \sqrt{\frac{1}{3}\operatorname{tr}(\boldsymbol{B}_B^*)} \tag{2.24}$$

The two remaining parameters that need to be determined through experimental tests are the initial stiffness of spring B, denoted C_R, and the locking stretch $\bar{\lambda}_L$.

2.2.3 Summary

All the parameters that have to be determined for the numerical material model are given in Table 2.1.

Table 2.1: Material parameters

Part A parameters

Spring

E	Young's modulus
ν	Poisson's ratio

Friction element

σ_T	Yield stress in tension
α	Ratio of yield stress in compression and tension
β	Parameter controlling plastic volumetric strain
σ_S	Saturation stress
H	Ramping parameter between σ_T and σ_S

Dashpot

$\dot{\varepsilon}_{0A}$	Reference strain rate
C	Strain rate sensitivity parameter

Part B parameters

Spring

C_R	Initial stiffness
$\bar{\lambda}_L$	Locking stretch

In addition, LS-DYNA requires the shear modulus G and the bulk modulus K to be input into this material model. These values can be calculated directly from Young's modulus and Poisson's ratio using these equations:

$$G = \frac{E}{2(1+\nu)} \tag{2.25}$$

$$K = \frac{E}{3(1-2\nu)} \tag{2.26}$$

2.3 Digital image correlation

This section will provide a description of digital image correlation (DIC), and how this can used for obtaining the strains from the experimental tests. The DIC program used in this study is called eCorr and was developed by Egil Fagerholt[8] at SIMLab. Digital image correlation is in essence the tracking of random patterns over a series of digital images. Spray-painting the test specimens with a black and white spotted pattern, and then taking a series of pictures during the tests, allows DIC to be used to obtain the strains of the specimens.

Using DIC, each pixel of the images is given a grayscale value between 0 and 255. The program then uses a correlation function to minimize the difference in grayscale values between the current and reference images. The DIC program used in this study, eCorr, uses a "finite element" type of mesh. Every element of the mesh has four nodes with two degrees of freedom each, as illustrated in Figure 2.11. The deformation of an element is governed by eight parameters, one for each degree of freedom, that have to be optimized in the correlation function. Using this type of element ensures a continuity of the displacement across element boundaries.[8]

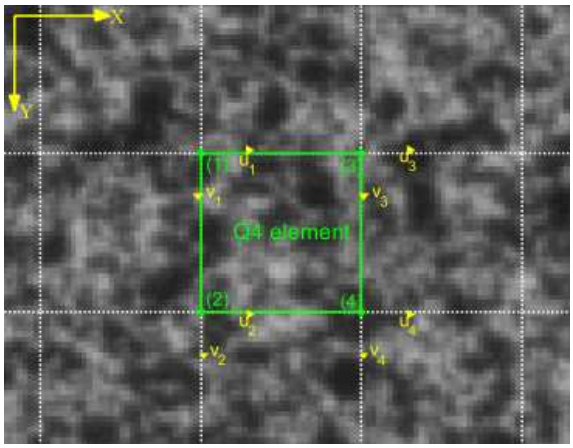

Figure 2.11: A Q4 element using the "finite element" DIC method[8]

A new feature of eCorr is 3D DIC. This method uses two cameras directed at the specimen, and the parts of the surface that are picked up by both cameras can be analyzed using 3D DIC. Given a camera calibration with information about the distances and angles between the specimen and the cameras, the program can combine the images from the two cameras into a 3D representation of the specimen. This is very useful for specimens with curved surfaces, or for materials that show a significant necking.

After the DIC analysis is completed for the whole image series, the strain history of selected elements can be written to a text file by eCorr.

Chapter 3

Experimental testing

Experimental tests were performed in order to determine the parameters describing the material behavior. These parameters were later used to accurately recreate the experiments in a finite element method simulation program. This chapter will describe the testing procedure and present the results obtained from the tests.

3.1 Materials and geometry

For this thesis, two different materials were tested, high-density polyethylene (HDPE) and polyvinyl chloride (PVC). For each material, three different specimen geometries were used, two for uniaxial tension and one for uniaxial compression. The first tension geometry is shown in Figure 3.1(a). This specimen has a gauge length of 4 mm and a quadratic cross section with sides of 6 mm, and will be called TQ (tension quadratic) is this thesis.

From previous tests performed with the TQ geometry, it has been observed that the corners of the cross section show a stiffer behavior than the middle. A new cylindrical geometry, shown in Figure 3.1(b), was therefore tested in order to eliminate this behavior and get a more uniform strain state. It has a 4 mm gauge length and a circular cross section with a diameter of 6 mm, and is called TC (tension circular).

The specimen used for compression is shown in Figure 3.1(c), it is a cylinder of height 10 mm and diameter 8 mm. It will be called CC (compression circular) for short.

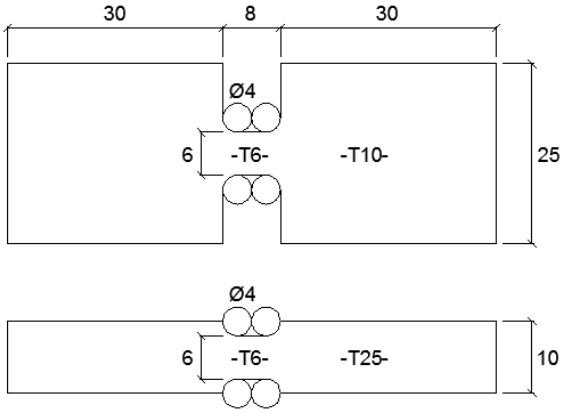

(a) TQ. Front and top faces

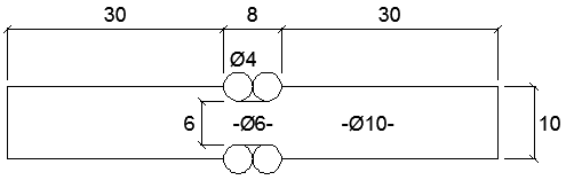

(b) TC

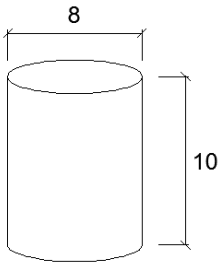

(c) CC

Figure 3.1: Geometries of test specimens

3.2 Test setup

All tests were carried out on a ZWICK/ROELL Z030 test machine. Determining the rate of displacement the machine should be set to, an initial strain rate of $\dot{\varepsilon}_0 = 10^{-2.5} s^{-1}$ was chosen. Using Equation (3.1), the velocity of the machine could be determined.

$$V = L_0 \times \dot{\varepsilon}_0 \tag{3.1}$$

where V is the velocity of the machine and L_0 is the initial gauge length of the specimen. A gauge length of 4 mm for the tension tests yielded a displacement velocity of 0.013 mm/s, while the 10 mm gauge length of the compression tests gave a velocity of 0.032 mm/s.

Some of the tension test specimens were subjected to cyclic loading. When the machine reached a given displacement, the direction of the displacement was reverted, using the same speed as before. When the force was equal to zero, the direction would be reverted again, continuing to pull in the tensile direction. This thesis will primarily focus on the monotonically loaded tests, and not that much on the cyclic tests.

Before each test, the specimen was spray-painted with a black and white spotted pattern so that the strains could later be retrieved using digital image correlation (DIC), as explained in Section 2.3. Figure 3.2 shows the test specimen in the machine and the placement of the cameras used for 3D DIC.

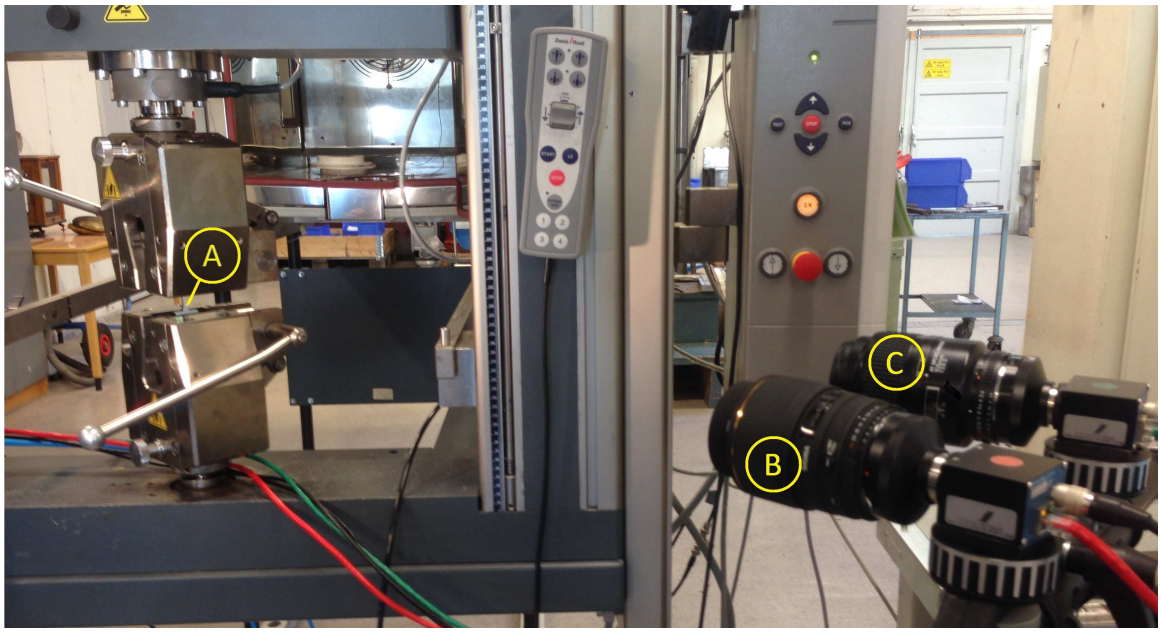

Figure 3.2: Camera setup for 3D DIC.
A: Test specimen
B: Camera 1
C: Camera 2

3.2.1 TQ

For HDPE, a total of six tests with geometry TQ were performed, with two different camera setups. The first four tests of the TQ specimens were performed with the two cameras directed at two perpendicular sides of the specimen. This would only allow for 2D DIC analysis to be performed on each side, but it would show if the non-quadratic handles of the specimens would affect the behavior of the sides of the gauge area. The last two tests were performed with two cameras directed at the same face of the specimens, this would allow for 3D DIC to be used for retrieving the strains of the specimens. Three of the tests were subjected to cyclic loading. The two camera setups are illustrated in Figure 3.3. Table 3.1 and Figure 3.4(a) shows which, and when loading was reverted.

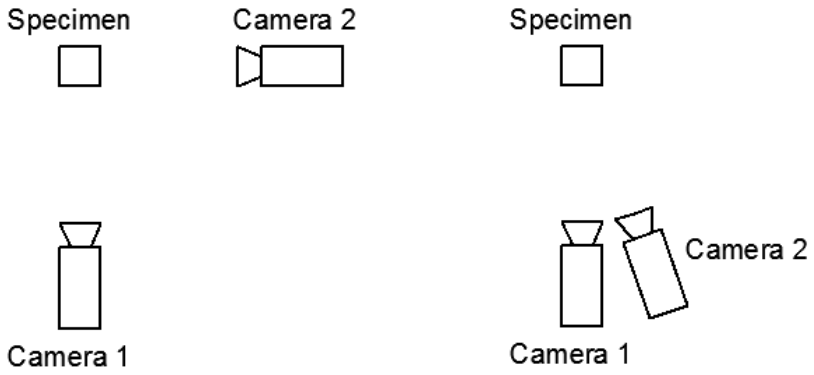

(a) 2D DIC (b) 3D DIC

Figure 3.3: Camera setups

Table 3.1: HDPE TQ tests

Test	DIC	Displacements where the loading was reverted
TQ-1	2D	Monotonic
TQ-2	2D	Monotonic
TQ-3	2D	36 mm
TQ-4	2D	5 mm, 15 mm, 25 mm, 35 mm
TQ-5	3D	Monotonic
TQ-6	3D	2.60 mm, 4.00 mm, 5.75 mm, 8.55 mm, 32.95 mm

Only the four first HDPE TQ tests were performed with cameras directed at two perpendicular sides. All other tests in this study had a camera setup for 3D DIC.

Five PVC tests with geometry TQ were performed. The first test did not have a satisfactory camera setup for DIC analysis and was therefore discarded. Of the four remaining tests, two were subjected to monotonic loading until failure and two were subjected to cyclic loading. Table 3.2 and Figure 3.4(b) shows the displacements where the loading was reverted for these tests. Based on the displacement at which the two monotonic tests reached failure, the last cycle was planned for around 9 mm. However, the cyclic tests failed long before the monotonic tests, and the last cycle could not be performed. The last cycle of test 5 was initiated after the force started dropping due to failure in the specimen.

Table 3.2: PVC TQ tests

Test	Displacements where the loading was reverted
TQ-2	Monotonic
TQ-3	Monotonic
TQ-4	1.2 mm, 1.8 mm, 2.5 mm, 4.0 mm
TQ-5	1.2 mm, 1.8 mm, 2.5 mm, 4.0 mm, 6.6 mm

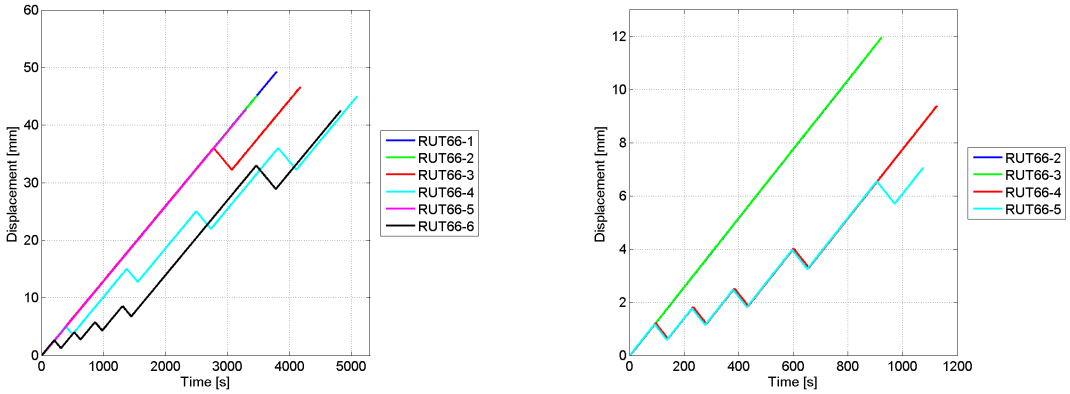

(a) HDPE

(b) PVC

Figure 3.4: Displacement history of TQ tests

3.2.2 TC

As this was a completely new specimen geometry, and there were only two specimens of each material, all tests were monotonically loaded until failure. It was preferable to have a backup monotonic test instead of running any cyclic tests with this geometry, in case the camera setup or lighting would disturb the DIC analysis.

3.2.3 CC

A problem with compression tests is the barreling effect. This happens because of the friction between the test machine and the specimen. The top and bottom of the specimen is held back from expanding in the transverse direction by this friction. The middle part of the specimen expands and gives it a barrel shape as seen in Figure 3.5. Several methods of reducing the friction by lubricating the specimen and machine have been tried, as is explained later in this section.

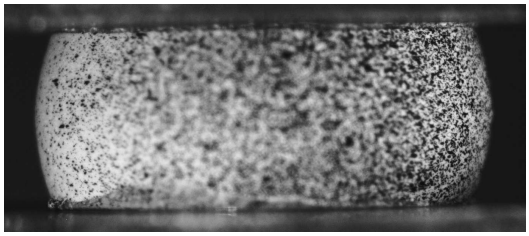

Figure 3.5: Barreling

Four PVC compression tests were performed. A displacement of about 7.35 mm were applied to all four specimens. The methods of reducing friction between the test machine and specimen is given in Table 3.3. Observing the two first tests, the edges of the specimens seemed to dig into the tape stuck to the machine. This could actually hold back the top and bottom faces from expanding, therefore one test with rounded edges was performed. As this did not make any noticeable difference, the last test was performed with the tape stuck directly onto the specimen.

Table 3.3: PVC CC tests

Test	Method of reducing friction
CC-1	Teflon tape on machine, oil on specimen
CC-2	Teflon tape on machine, oil on specimen
CC-3	Teflon tape on machine, oil on specimen, rounded edges
CC-4	Teflon tape on specimen

Three HDPE compression tests were performed. The method of reducing friction from the last PVC test of using teflon tape directly on the specimen worked quite well. All the HDPE tests have therefore been performed in this manner, in addition to lubricating the surfaces of the test machine with oil. All tests were loaded monotonically to a given displacement, at which point they were unloaded. Table 3.4 shows the maximum displacement of the different tests.

Table 3.4: HDPE CC tests

Test	Maximum displacement
CC-1	6.58 mm
CC-2	7.02 mm
CC-3	8.49 mm

3.3 Post-processing

For all the experimental tests, the procedure of obtaining the time histories of the displacement, force, strain and stress were done in a similar manner. The force and displacement were logged and written to a file by the test machine. The longitudinal and transverse strains were obtained using the DIC program eCorr. Later, the transverse strains from the DIC analysis were used to find the cross section area, and from this the stress was determined.

3.3.1 DIC

This was the first time 3D DIC had been used with eCorr, but it worked very well. In addition to the usual 2D image results seen in Figures 3.6(a) and (b), these images were combined into a 3D representation of the specimen surface seen in Figure 3.6(c).

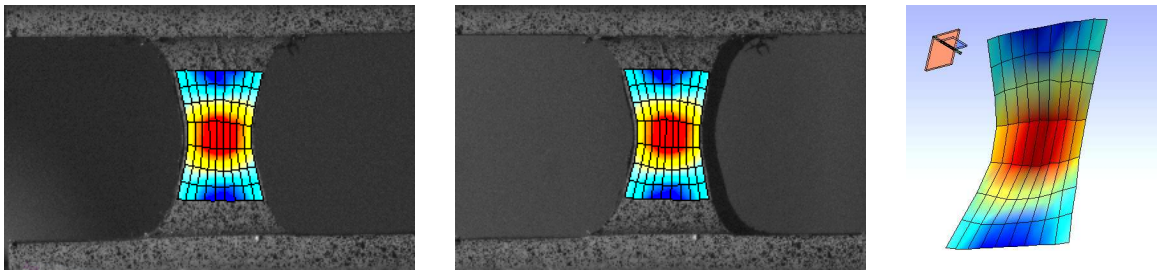

(a) Camera 1 (b) Camera 2 (c) 3D

Figure 3.6: Images from test HDPE TQ-5 and the resulting 3D strain field map

As can be seen in Figure 3.6(c), 3D DIC captures the curvature away from the camera at necking, which cannot be picked up by a single camera. Especially for HDPE, where there is a significant contraction at necking, this difference can have a significant effect on the results.

For the tension tests, only the strains of the elements at the neck were used for further calculations. For the compression tests, some elements from the middle of the specimens were used, see Figure 3.7.

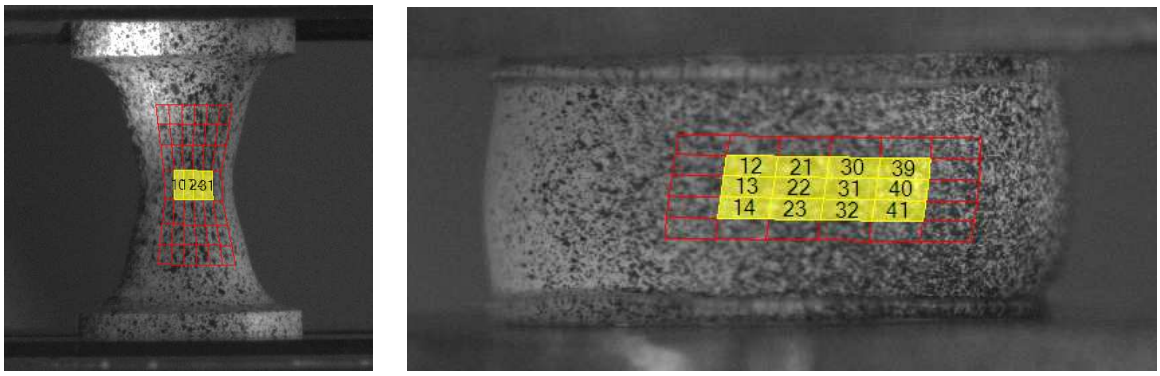

(a) HDPE TC-1 (b) PVC CC-2

Figure 3.7: Elements from which strains were obtained

As far as it was possible, all 12 elements from Figure 3.7(b) were used. Towards the end of some of the tests, a few of these elements were extremely deformed because the program was not able to correctly track the pattern on the specimens. In these cases, only the elements that remained close to rectangular were selected.

The longitudinal strains ε_l and transverse strains ε_t from the selected elements were written directly to a text file by eCorr.

3.3.2 Further processing

After writing the longitudinal and transverse strains from eCorr to a file, Matlab was used to further process the results. The transverse strains were used to calculate a time history of the cross section area at necking. For the quadratic TQ geometry, Equation (3.2) was used.

$$A = d_0^2 \times e^{\varepsilon_t} \times e^{\varepsilon_t} \tag{3.2}$$

where $d_0 = 6mm$ is the initial side length.

Deriving an equation for the area of the cylindrical specimens TC and CC started with the relation between the radius r, angle θ and arc length S, given as:

$$r\theta = S \tag{3.3}$$

Assuming that the sector covered by the elements has a constant angle throughout the tests we get

$$\theta = \frac{S_0}{r_0} = \frac{S}{r} \tag{3.4}$$

where r_0 and S_0 are the initial radius and arc length respectively, see Figure 3.8

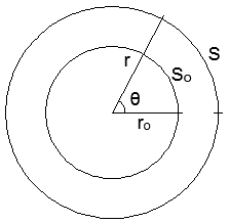

Figure 3.8: Variables in Equation (3.4)

The arc length S can be defined by the initial length multiplied by the transverse strain:

$$S = S_0 \times e^{\varepsilon_t} \tag{3.5}$$

Equation (3.4) can then be rewritten as:

$$\frac{S_0}{r_0} = \frac{S_0 \times e^{\varepsilon_t}}{r}$$

$$r = r_0 \times e^{\varepsilon_t} \tag{3.6}$$

From Equation (3.6), an equation for the cross section area is obtained:

$$A = \pi \times r_0^2 \times e^{\varepsilon_t} \times e^{\varepsilon_t} \tag{3.7}$$

where $r_0 = 3mm$ and $r_0 = 4mm$ are the initial radii of TC and CC respectively.

Using the force history taken directly from the test machine and the cross section area calculated from Equation (3.7), the true stress can be found using Equation (3.8)

$$\sigma = \frac{F}{A} \tag{3.8}$$

In order to determine the volumetric strain of the test, the area strain is first found using Equation (3.9)

$$\varepsilon_A = \ln \frac{A}{A_0} \tag{3.9}$$

Summing the longitudinal and area strains then gives the volumetric strain:

$$\varepsilon_V = \varepsilon_l + \varepsilon_A \tag{3.10}$$

Chapter 4

Results from experimental tests

In this chapter, the results of all the experimental tests will be presented, accompanied by short discussions. These results will provide the basis of the calibration of the numerical model, which will be explained in detail in Chapter 5.

4.1 HDPE

4.1.1 Tension tests

The test setup for 2D DIC had two cameras directed at two perpendicular sides of the specimen. The most relevant result from these tests is whether the two perpendicular sides have the same behavior. Figure 4.1 shows curves of the transverse strain plotted against the longitudinal strain for two of the tests.

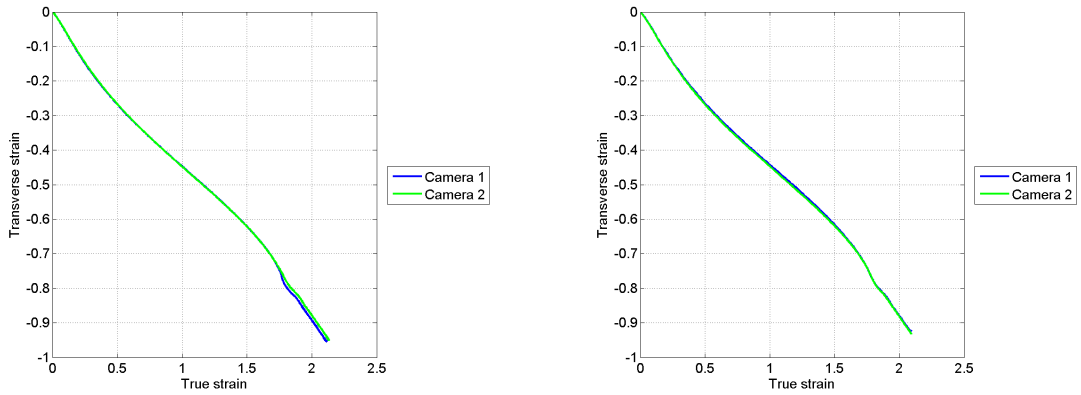

(a) TQ-1 (b) TQ-2

Figure 4.1: Transverse vs. longitudinal strains for perpendicular sides of two TQ specimens

The curves show that two perpendicular sides of the specimen deform identically, and that the gauge section's behavior is not affected by the shape of the handles of the specimen. This can therefore also be assumed for the 3D tests, where the cameras were directed at only one side.

The resulting force-displacement curves of all HDPE TQ tests are shown in Figure 4.2. For better visibility of the curves, they have been split into two plots, one

with the 2D tests and one with the 3D tests. There is practically no spread in the results of the monotonic tests.

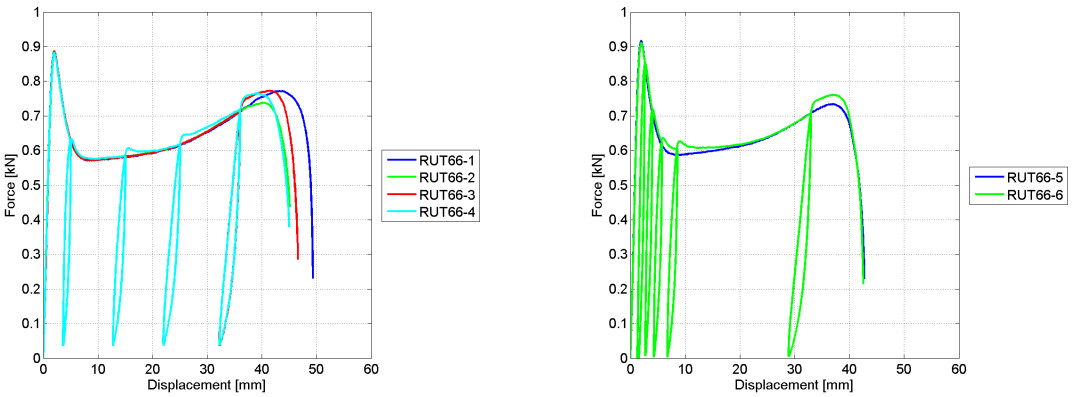

(a) 2D tests

(b) 3D tests

Figure 4.2: Force-displacement curves from HDPE TQ tests

For the cyclically loaded tests, the force is greater than that of the monotonic tests right after each cycle . After being stretched a bit further, the cyclic tests again stabilize exactly at the monotonic curve. All the tests also fracture at about the same displacement, so the unloading does not seem to affect the capacity of the material.

The stress-strain curves of the HDPE TQ tests are given in Figure 4.3. Comparing Figure 4.2(a) and 4.3(a), it can be seen that use of regular intervals of displacement for the unloading cycles yields a stress-strain curve where almost all cycles are pushed towards the end of the curve. Figure 4.4 was then used to determine which displacements would give a stress-strain curve where the cycles are evenly spread out. The 3D cyclic test TQ-6 was performed using these displacement values.

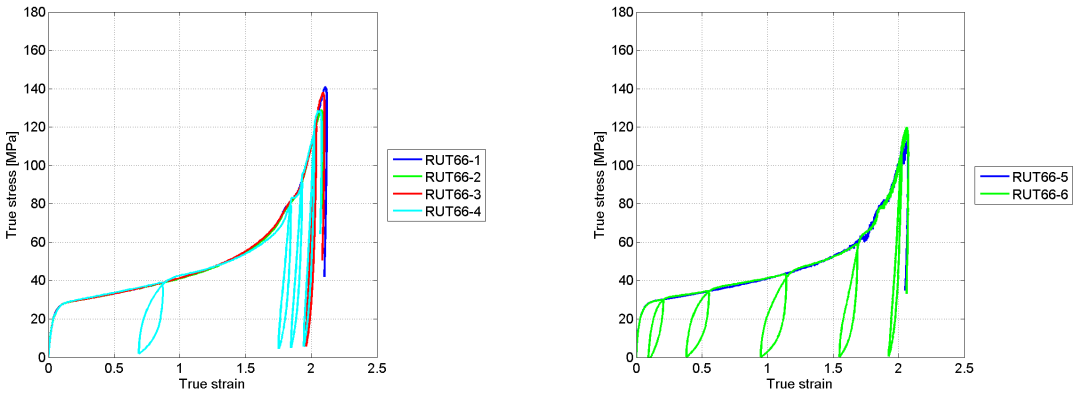

(a) 2D tests (b) 3D tests

Figure 4.3: Stress-strain curves from HDPE TQ tests

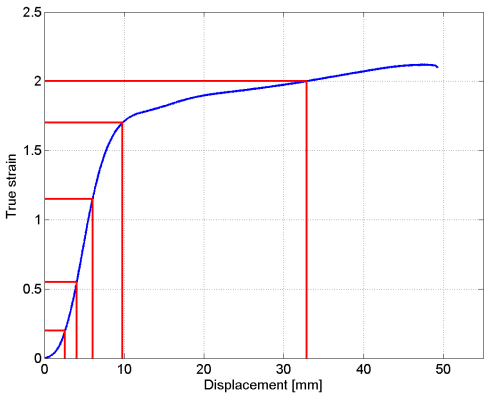

Figure 4.4: True strain plotted against displacement for TQ-1

The results of the HDPE TC tests are shown in Figure 4.5. The two tests have yielded exactly the same results, this indicates that the 3D DIC camera calibration is accurate and works very well for these cylindrical specimens. Since the initial cross section area of the TC geometry is smaller than that of TQ, these tests reach yielding at a lower force. But they also appear to reach a higher stress before failure than TQ did.

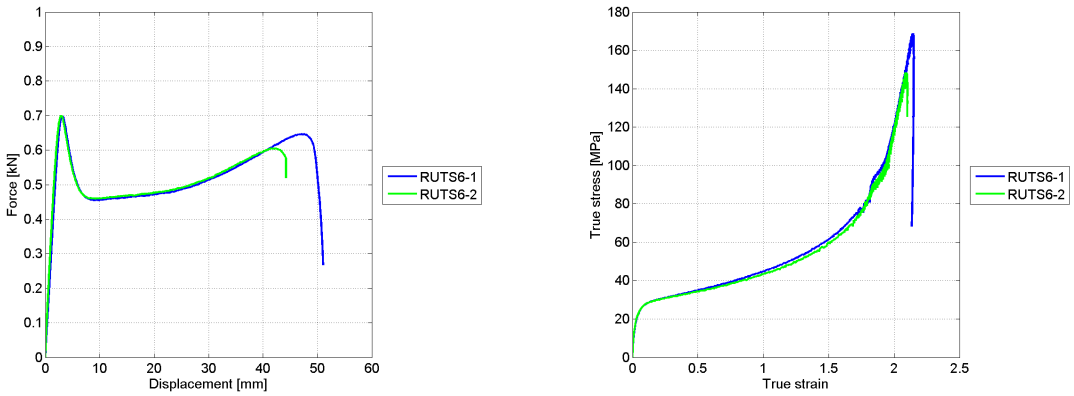

(a) Force-displacement (b) Stress-strain

Figure 4.5: Force-displacement and stress-strain curves from HDPE TC tests

4.1.2 Compression tests

The resulting force-displacement and stress-strain curves from the HDPE compression tests are shown in Figure 4.6.

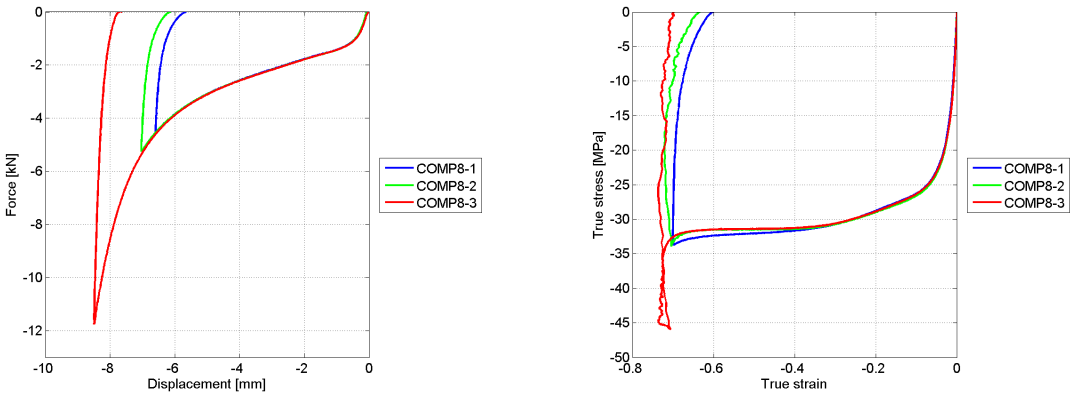

(a) Force-displacement (b) Stress-strain

Figure 4.6: Force-displacement and stress-strain curves from HDPE compression tests

The first two tests were compressed from the initial 10 mm to about 3 mm in height, the last test was compressed to less than 2 mm in height. This difference doubled the maximum applied force. From the stress-strain curve, it can be seen that the strain does not increase at all due to the extra displacement in the last test; this can clearly not be true. A maximum strain of -0.7, which all three tests show, is also very small for a compression from 10 to 3 mm. Basing the strain on the displacement instead of

the DIC results, the maximum strain should in this case be:

$$\varepsilon = \ln \frac{L}{L_0} = \ln \frac{3}{10} = -1.2 \tag{4.1}$$

which is significantly larger than the strain of -0.7 obtained from the DIC analysis. Figure 4.7(a) shows the difference in the strain time history of the compression tests when the strains are based on the displacement compared to DIC analysis. Calculating the strain from the displacements, the maximum strain of the tests becomes lager, and they differ from each other based on how much the specimens were compressed. This makes a lot more sense than the strains all flattening out at -0.7, and a longitudinal strain measure based on the displacement will be used on the compression tests from here on. The area of the specimens will still be determined from the transverse strains obtained through DIC analysis.

New stress-strain curves, where the strain is determined using the displacement, are shown in Figure 4.7(b), also comparing them to the old curves based on DIC.

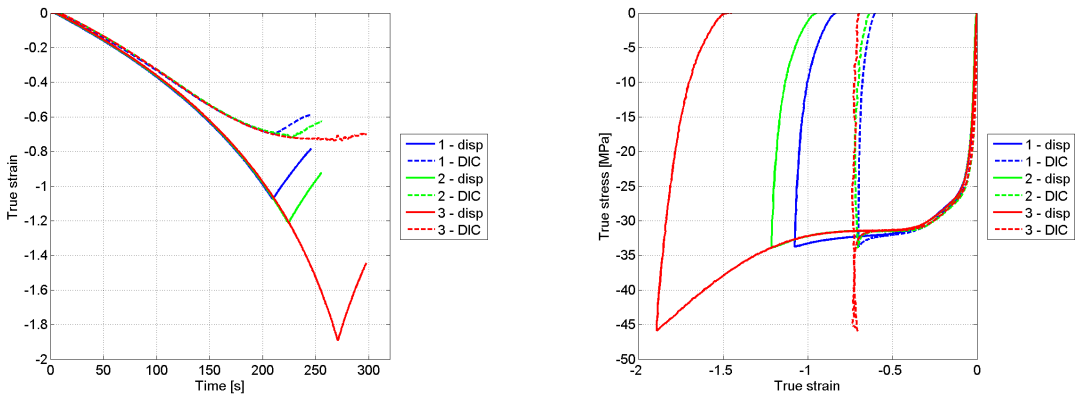

(a) Longitudinal strain

(b) Stress-strain

Figure 4.7: Comparison of the strain history and stress-strain curves, with strains based on both displacement and DIC

The reason for the large error in the strains from DIC analysis is likely due to barreling. When the middle section of the specimens bend outwards, the surface here is no longer directly under the applied force. The surface is therefore less compressed than the internal parts of the specimen. The barreling effect is so large towards the end of the tests that the upper and lower parts of the specimens' sides become horizontal and is directly pushed on by the test machine. While the parts of the sides that can still be seen are only pushed outward and is not further compressed in the longitudinal direction, the internal parts of the specimens are subjected to very large strains. Only observing the surface of the compression specimens therefore does not give an

accurate picture of what happens inside. The barreling effect is illustrated in Figure 4.8.

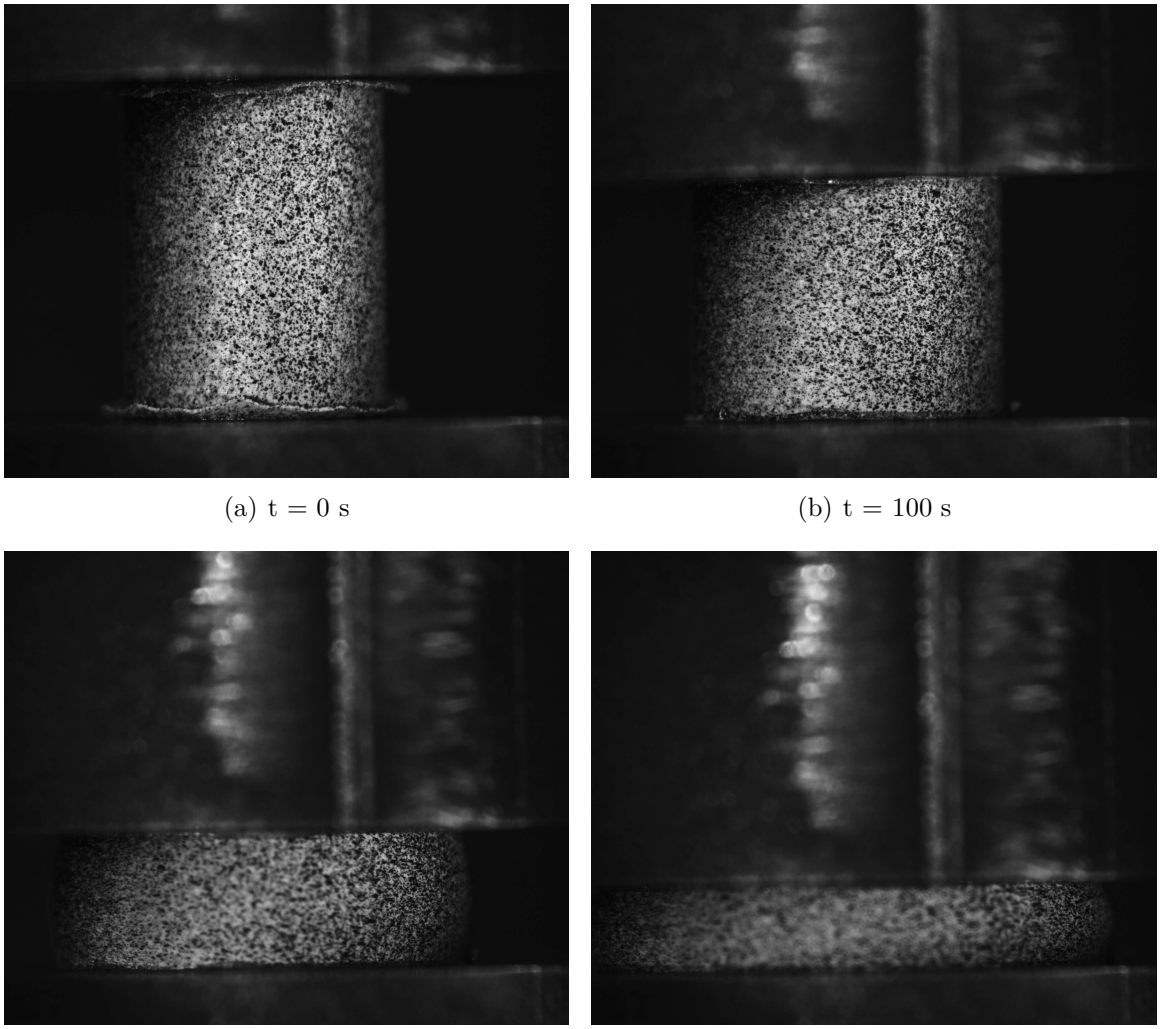

(a) t = 0 s (b) t = 100 s

(c) t = 200 s (d) t = 250 s

Figure 4.8: HDPE compression test 3 at different times

4.1.3 Comparison of geometries

In order to give a better comparison of the results from the different geometries, Figure 4.9 shows TQ-5, TC-1 and CC-3 in the same plots. Since the other tests for each geometry yield very similar results, these three tests will represent each geometry for the rest of the thesis.

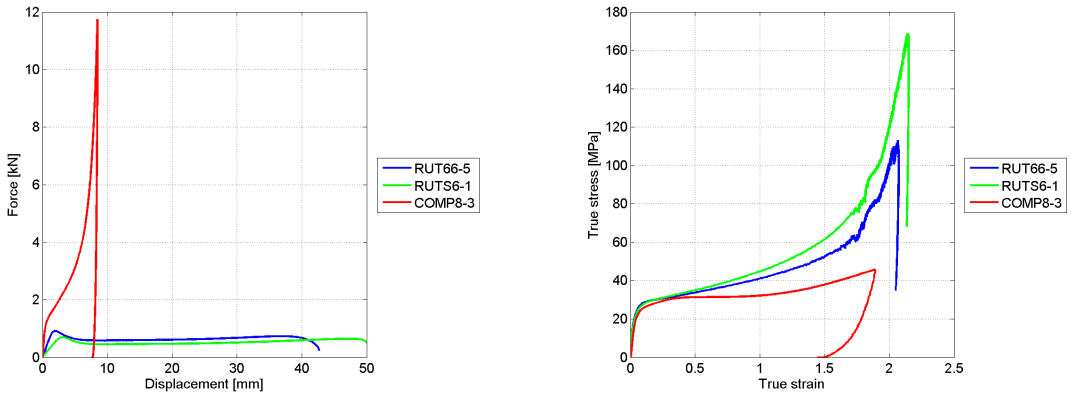

(a) Force-displacement

(b) Stress-strain

Figure 4.9: Comparison of force-displacement and stress-strain curves for the different geometries of HDPE

The difference in the stress-strain curves in tension and compression can be explained from the molecular structure of the material. Since the long polymer chains are not stretched out in compression, these tests will not reach a locking stretch where the strain ceases. Note that the stress-strain relationship in tension seems to be affected by which geometry is used; this will be discussed further in Chapter 6.

The last plots that will be discussed here are the volumetric strains. In Figure 4.10(a), a time history of the volumetric strain is plotted for the three different geometries. The same three tests are shown in Figure 4.10(b), but here the volumetric strain is plotted against the longitudinal strain. For both tension geometries, there is a negative volumetric strain in the elastic part of the curve, which is a very counterintuitive result. Normally, the volume of a material subjected to tensile loading will either increase or stay roughly the same, but HDPE seems to decrease in volume in the beginning of the tensile tests. As with the stress-strain curve, the results from two tension geometries differ here.

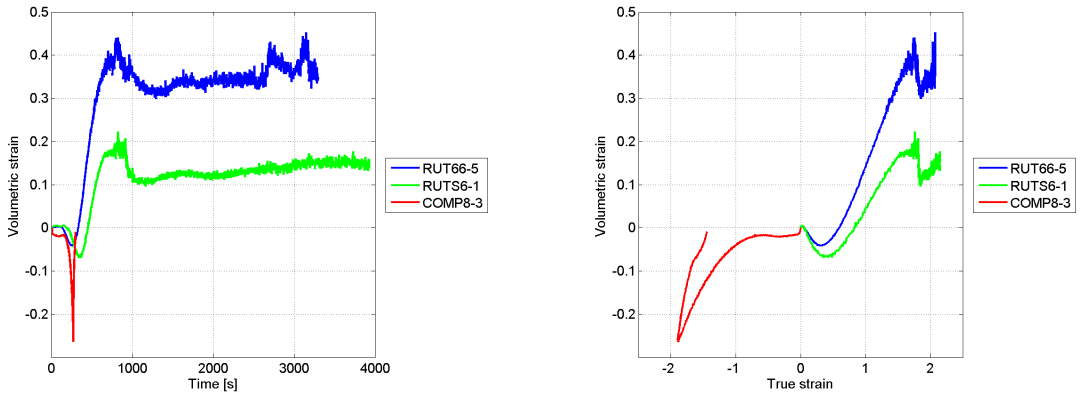

(a) Volumetric strain time history

(b) Volumetric vs. longitudinal strain

Figure 4.10: Volumetric strain of HDPE tests

4.2 PVC

Here, the results from the PVC experimental tests are presented. The calibration of PVC for the numerical model done in Section 5.4, will be based on these results.

4.2.1 Tension tests

In Figure 4.11, the force-displacement and stress-strain curves of the TQ tests are shown. As with HDPE, the cyclically loaded tests go back to the monotonically loaded curves after each cycle. With PVC, however, the cyclic tests reached failure before the monotonic tests, one at just half the displacement of the monotonic tests. Since only four tests were performed, two monotonic and two cyclic, this could just be random. More tests would have to be performed in order to determine whether the unloading affects the material's capacity.

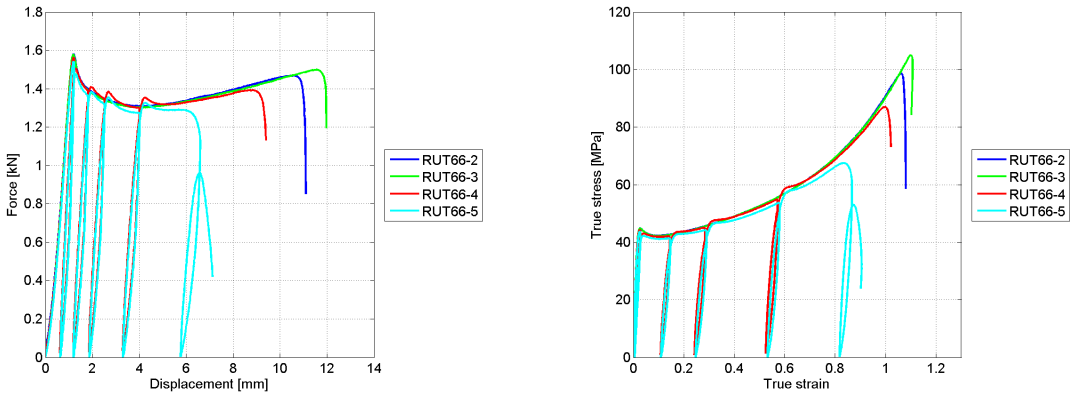

(a) Force-displacement (b) Stress-strain

Figure 4.11: Force-displacement and stress-strain curves from PVC TQ tests

As with HDPE, the PVC TC specimens' behavior match exactly, see Figure 4.12. The maximum force of both tension geometries is larger for PVC than HDPE, but the PVC fractures at a much smaller displacements than HDPE. This shows that PVC has a higher strength, but lower ductility than HDPE. From Figures 4.11(b) and 4.12(b), it can be seen that PVC has a yield stress σ_T that is larger than the saturation stress σ_S, which means this material softens after yielding.

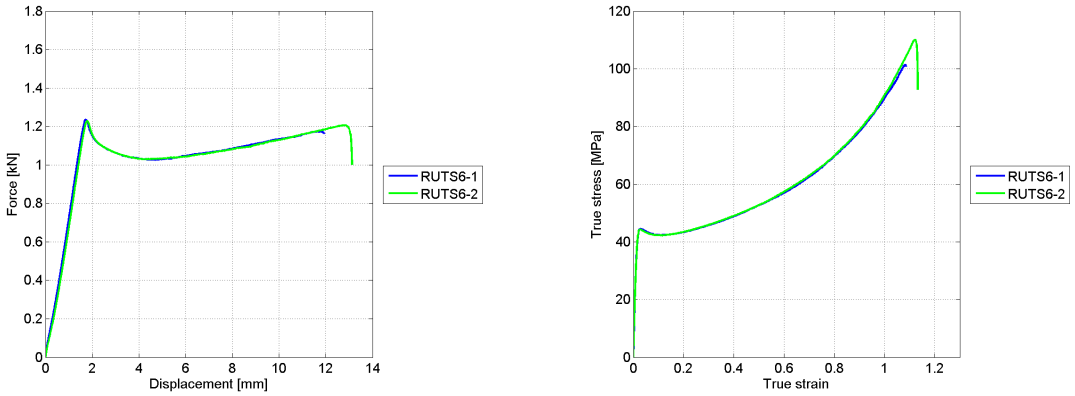

(a) Force-displacement (b) Stress-strain

Figure 4.12: Force-displacement and stress-strain curves from PVC TC tests

4.2.2 Compression tests

The PVC compression tests suffered the same problem as HDPE with the longitudinal strains from DIC. Figure 4.13 shows a time history of strains calculated from

displacements and strains taken directly from DIC analysis. Figure 4.14 shows the force-displacement and stress-strain curves from the PVC compression tests.

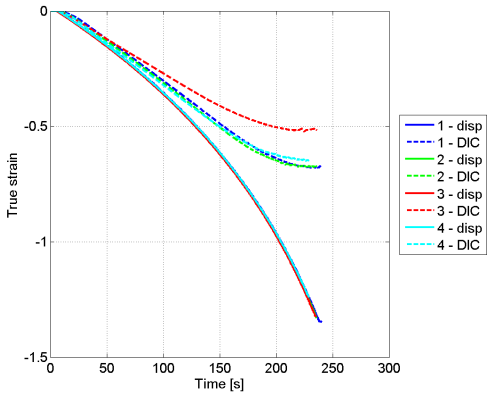

Figure 4.13: Comparison of the strain time history with strains based on both displacement and DIC

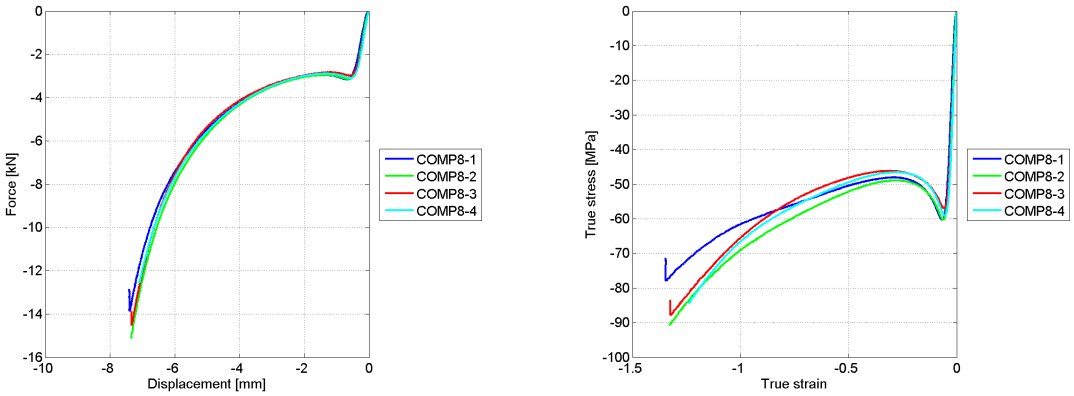

(a) Force-displacement

(b) Stress-strain

Figure 4.14: Force-displacement and stress-strain curves from PVC compression tests

4.2.3 Comparison of geometries

Comparing the different PVC geometries in Figure 4.15, it can be seen that, unlike HDPE, the two tension geometries here match up perfectly. The compression test also has a much larger yield stress than the tension geometries.

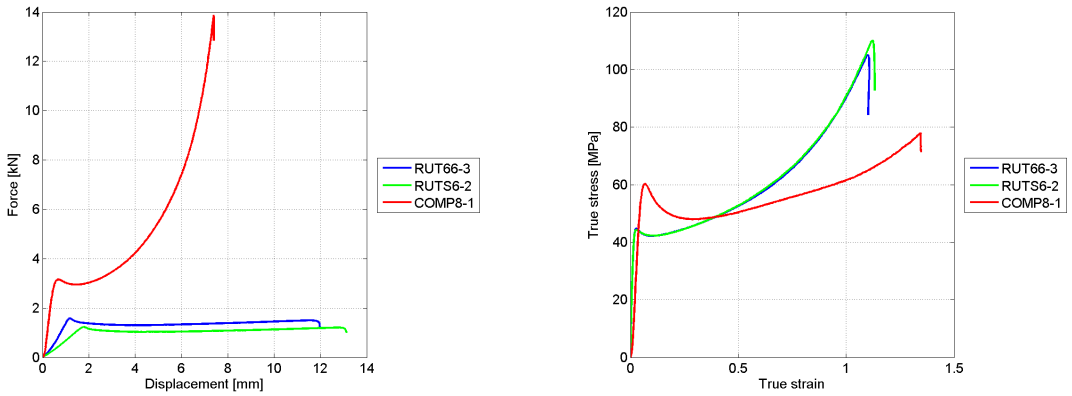

(a) Force-displacement (b) Stress-strain

Figure 4.15: Comparison of force-displacement and stress-strain curves for the different geometries of PVC

The curves for the volumetric strain in Figure 4.16 shows that there is no negative volumetric strain in tension for PVC. The two tension geometries are also more consistent here than for HDPE.

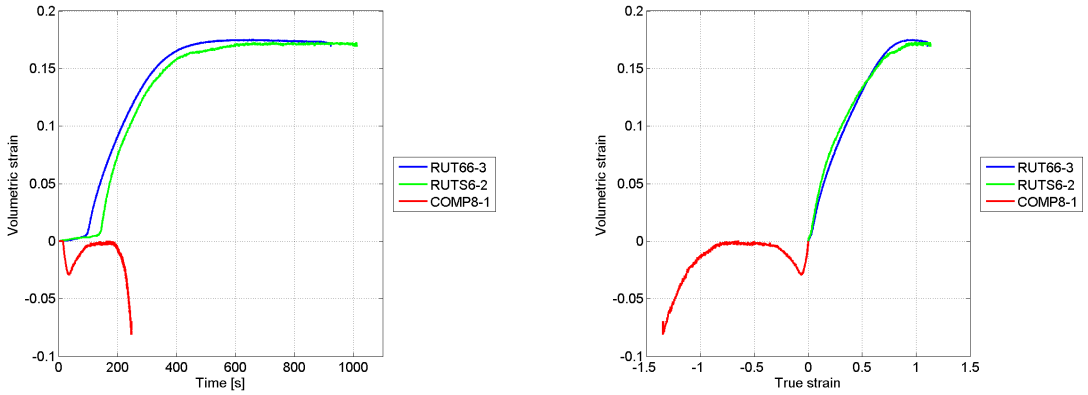

(a) Volumetric strain time history (b) Volumetric vs. longitudinal strain

Figure 4.16: Volumetric strain of PVC tests

Chapter 5

Calibration of material model

Based on the experimental results, the material parameters from Table 2.1 had to be determined. The calibration is primarily done by observing the results of the tensile tests, except for α, where the yield strength in compression is needed.

5.1 Part A parameters

5.1.1 Spring

The initial stiffness given by Young's modulus is simply determined by finding the initial slope of the stress-strain curves from Chapter 4, using Equation (5.1)

$$E = \frac{d\sigma}{d\varepsilon} \tag{5.1}$$

Poisson's ratio ν is defined by Equation (5.2) as the ratio of the transverse and longitudinal strain in the elastic domain, i.e. up to a longitudinal strain of about 0.2

$$\nu = -\frac{\varepsilon_l^e}{\varepsilon_t^e} \tag{5.2}$$

A plot of this ratio against the longitudinal strain will give the value of Poisson's ratio by observing the curve in the elastic domain.

5.1.2 Friction element

The method for determining the yield stress in tension σ_T, is different depending on whether the material hardens or softens after yielding. As seen in Figure 2.10, a material that softens has a very clear yield stress that is easy to determine by reading the maximum value of the stress-strain curve. For materials that harden, the transition from elasticity to plasticity is more diffuse. Using the stress at 0.2 % plastic strain as the yield stress is common for materials that do not have a very clear yield stress. This has therefore been done for HDPE here, it is found by plotting a line parallel to the Young's modulus shifted 0.002 on the strain axis, and see where it intersects the stress-strain curve.

In order to obtain a value for α, the yield stress in compression σ_C has to be determined. This is done in exactly the same way as σ_T, only using the stress-strain

curves from the compression tests. The values of σ_C and σ_T is then used in Equation (2.14) to calculate α.

The parameter β controls the volumetric strain in the plastic domain of deformation. It is related to a retraction ratio ρ, which is defined the same way as Poisson's ratio from Equation (5.2), only in the plastic domain:

$$\rho = -\frac{\varepsilon_2^p}{\varepsilon_1^p} \tag{5.3}$$

where ε_1^p and ε_2^p are the principal plastic strains. The relation between β and ρ can be derived from the principle of maximum plastic dissipation, which results in Equation (5.4) [5]

$$\dot{\boldsymbol{\varepsilon}}^p = \dot{\lambda}\frac{\delta g}{\delta \boldsymbol{\sigma}} \tag{5.4}$$

The plastic strain rate matrix $\dot{\boldsymbol{\varepsilon}}^p$ for uniaxial tension is given as

$$\dot{\boldsymbol{\varepsilon}}^p = \begin{bmatrix} \dot{\varepsilon}_1^p & 0 & 0 \\ 0 & \dot{\varepsilon}_2^p & 0 \\ 0 & 0 & \dot{\varepsilon}_3^p \end{bmatrix} = \dot{\varepsilon}_1^p \begin{bmatrix} 1 & 0 & 0 \\ 0 & -\rho & 0 \\ 0 & 0 & -\rho \end{bmatrix} \tag{5.5}$$

For the uniaxial case, $\dot{\lambda} = \dot{\varepsilon}_1^p$ also applies. The last part of Equation (5.4) is the derivative of the plastic potential in Equation (2.18). This can be broken down into

$$\frac{\delta g}{\delta \boldsymbol{\sigma}} = \frac{\partial g}{\partial I_1}\frac{\partial I_1}{\partial \boldsymbol{\sigma}} + \frac{\partial g}{\partial J_2}\frac{\partial J_2}{\partial \boldsymbol{\sigma}} \tag{5.6}$$

and each part is then calculated:

$$\frac{\partial g}{\partial I_1} = \frac{\beta - 1}{2\beta} + \frac{(\beta-1)^2 I_1}{2\beta\sqrt{(\beta-1)^2 I_1^2 + 12\beta J_2}} \tag{5.7}$$

$$\frac{\partial g}{\partial J_2} = \frac{3}{\sqrt{(\beta-1)^2 I_1^2 + 12\beta J_2}} \tag{5.8}$$

I_1 and J_2 are the invariants from Equations (2.11) and (2.12); their derivatives are given as:

$$\frac{\partial I_1}{\partial \boldsymbol{\sigma}} = \begin{bmatrix} 1 & 0 & 0 \\ 0 & 1 & 0 \\ 0 & 0 & 1 \end{bmatrix} \tag{5.9}$$

$$\frac{\partial J_2}{\partial \boldsymbol{\sigma}} = \frac{\sigma}{3}\begin{bmatrix} 2 & 0 & 0 \\ 0 & -1 & 0 \\ 0 & 0 & -1 \end{bmatrix} \tag{5.10}$$

In uniaxial tension, the invariants I_1 and J_2 takes on the values

$$I_1 = \sigma \tag{5.11}$$

$$J_2 = \frac{1}{3}\sigma^2 \tag{5.12}$$

Combining Equations (5.11) and (5.12) with Equations (5.7) and (5.8) yields:

$$\frac{\partial g}{\partial I_1} = \frac{\beta - 1}{2\beta} + \frac{(\beta-1)^2 \sigma}{2\beta\sqrt{(\beta-1)^2\sigma^2 + 4\beta\sigma^2}} = \frac{\beta-1}{2\beta} + \frac{(\beta-1)^2}{2\beta(\beta+1)} = \frac{\beta-1}{\beta+1} \tag{5.13}$$

$$\frac{\partial g}{\partial J_2} = \frac{3}{\sqrt{(\beta-1)^2\sigma^2 + 4\beta\sigma^2}} = \frac{3}{\sigma(\beta+1)} \tag{5.14}$$

Inserting all the parts back into Equation (5.6) gives the expression:

$$\frac{\delta g}{\delta \bar{\sigma}} = \frac{\beta-1}{\beta+1}\begin{bmatrix}1 & 0 & 0\\ 0 & 1 & 0\\ 0 & 0 & 1\end{bmatrix} + \frac{1}{\beta+1}\begin{bmatrix}2 & 0 & 0\\ 0 & -1 & 0\\ 0 & 0 & -1\end{bmatrix} \tag{5.15}$$

Equation (5.4) can now be rewritten as:

$$\begin{bmatrix}1 & 0 & 0\\ 0 & -\rho & 0\\ 0 & 0 & -\rho\end{bmatrix} = \frac{\beta-1}{\beta+1}\begin{bmatrix}1 & 0 & 0\\ 0 & 1 & 0\\ 0 & 0 & 1\end{bmatrix} + \frac{1}{\beta+1}\begin{bmatrix}2 & 0 & 0\\ 0 & -1 & 0\\ 0 & 0 & -1\end{bmatrix} \tag{5.16}$$

Using the two bottom equations, the relation between β and ρ is obtained:

$$-\rho = \frac{\beta-1}{\beta+1} - \frac{1}{\beta+1} = \frac{\beta-2}{\beta+1} \tag{5.17}$$

$$\beta = \frac{2-\rho}{1+\rho} \tag{5.18}$$

Just like the yield stress, the saturation stress σ_S is determined differently depending on whether the material hardens or softens after yielding. For the softening case, there is an easily obtainable local minimum on the stress-strain curve that can be used as σ_S. By this time in the test, part B stress will also affect the total stress of the material, thus σ_S will be overestimated using this method. Even though it is not an accurate value for the saturation stress, it an okay initial value which can be adjusted using inverse modeling and curve fitting. For the case of hardening materials, Considère's criterion is used to determine σ_S[4]. This criterion is used to find the point where necking starts for materials with diffuse necking. It is given as

$$f(\lambda, \sigma) = \lambda - \frac{\delta\lambda}{\delta\sigma}\sigma = 0 \tag{5.19}$$

where the stretch λ is defined as

$$\lambda = e^{\varepsilon_l} \tag{5.20}$$

This criterion locates the point where the tangent of the stretch-stress curve goes through the origin of the σ-λ plane, as illustrated in Figure 5.1.

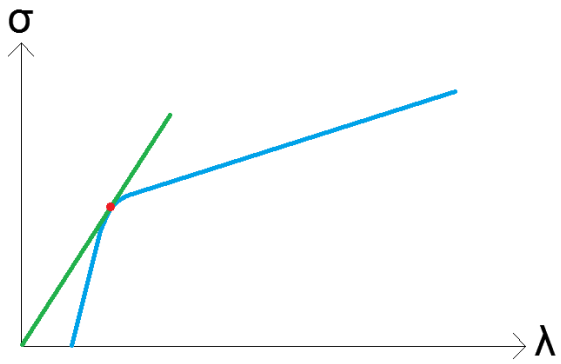

Figure 5.1: Considère's criterion

The ramping parameter H is determined using Equation (2.19) with a target plastic strain $\varepsilon^p_{A,S}$ where the saturation stress σ_S is reached. Since the stress will go towards σ_S, but never actually reach it, Hovden[4] proposes that 95% of the transition from yield to saturation stress should be completed at the target strain. In other words, this means that Equation (2.19) can be written as:

$$R = (\sigma_S - \sigma_T)\left[1 - \exp\left(-H\varepsilon^p_{A,S}\right)\right] = 0.95\,(\sigma_S - \sigma_T) \tag{5.21}$$

which gives

$$\begin{aligned}\left[1 - \exp\left(-H\varepsilon^p_{A,S}\right)\right] &= 0.95 \\ \exp\left(-H\varepsilon^p_{A,S}\right) &= 0.05 \\ H &= -\frac{\ln 0.05}{\varepsilon^p_{A,S}}\end{aligned} \tag{5.22}$$

A value for the target plastic strain $\varepsilon^p_{A,S}$ cannot be obtained directly from the experimental results. In this thesis, an estimate has been set by subtracting the strain at yielding from the strain at the saturation stress.

5.1.3 Dashpot

Since all the experimental tests in this study were performed at the same strain rate, the results are inadequate for directly determining the rate dependent parameters $\dot{\varepsilon}_{0A}$ and $C(\theta)$. Hovden[4] performed experiments with different strain rates for both materials for his master thesis. His values for rate dependence has therefore been used also for this thesis.

5.2 Part B parameters

The part B parameters C_R and $\bar{\lambda}_L$, initial stiffness and locking stretch respectively, are best determined through inverse modeling. An estimate of the locking stretch can however be obtained. Calculating the distortional part of the deformation gradient from Section 2.2 yields

$$\boldsymbol{F}_B^* = J_B^{-1/3}\boldsymbol{F}_B = J_B^{-1/3}\begin{bmatrix}\lambda_1 & 0 & 0\\ 0 & \lambda_2 & 0\\ 0 & 0 & \lambda_2\end{bmatrix} \tag{5.23}$$

The distortional left Cauchy-Green deformation tensor then becomes

$$\boldsymbol{B}_B^* = \boldsymbol{F}_B^*\left(\boldsymbol{F}_B^*\right)^T = J_B^{-\frac{2}{3}}\begin{bmatrix}\lambda_1^2 & 0 & 0\\ 0 & \lambda_2^2 & 0\\ 0 & 0 & \lambda_2^2\end{bmatrix} \tag{5.24}$$

where the Jacobian is given by Equation (2.2) as

$$J_B = \det(\boldsymbol{F}_B) = \lambda_1\lambda_2^2 \tag{5.25}$$

Equation (2.24) can then be rewritten as

$$\bar{\lambda} = \sqrt{\frac{1}{3}\operatorname{tr}\left(\boldsymbol{B}_B^*\right)} = \sqrt{\frac{1}{3}J_B^{-\frac{2}{3}}\left(\lambda_1^2+2\lambda_2^2\right)} = \sqrt{\frac{1}{3}\left(\lambda_1\lambda_2^2\right)^{-\frac{2}{3}}\left(\lambda_1^2+2\lambda_2^2\right)} \tag{5.26}$$

Using the relation between stretch and strain from Equation (5.20) gives

$$\bar{\lambda} = \sqrt{\frac{1}{3}\left\{\exp\left[-\frac{2}{3}\left(\varepsilon_1+2\varepsilon_2\right)\right]\left[\exp\left(2\varepsilon_1\right)+2\exp\left(2\varepsilon_2\right)\right]\right\}} \tag{5.27}$$

$$\bar{\lambda} = \sqrt{\frac{1}{3}\left\{\exp\left[\frac{4}{3}\left(\varepsilon_1-\varepsilon_2\right)\right]+2\exp\left[-\frac{2}{3}\left(\varepsilon_1-\varepsilon_2\right)\right]\right\}} \tag{5.28}$$

Introducing locking strain ε_L, and using the relation between transverse and longitudinal strain from Equation (5.3) gives an expression for the locking stretch $\bar{\lambda}_L$:

$$\bar{\lambda}_L = \sqrt{\frac{1}{3}\left\{\exp\left[\frac{4}{3}\varepsilon_{1,L}\left(1+\rho\right)\right]+2\exp\left[-\frac{2}{3}\varepsilon_{1,L}\left(1+\rho\right)\right]\right\}} \tag{5.29}$$

Now, only the longitudinal locking strain has to be determined from the experimental results.

5.3 Calibration of HDPE

5.3.1 Part A

Starting with the Young's modulus E, it can be seen from Figure 5.2 that there is a difference between the 2D and 3D DIC results. The calibration of E is based on the 3D results, which has a steeper slope. A Young's modulus of 1400 MPa is shown to be a good fit in Figure 5.3.

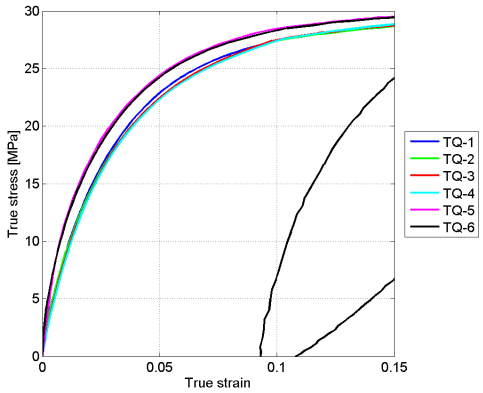

Figure 5.2: HDPE TQ tests

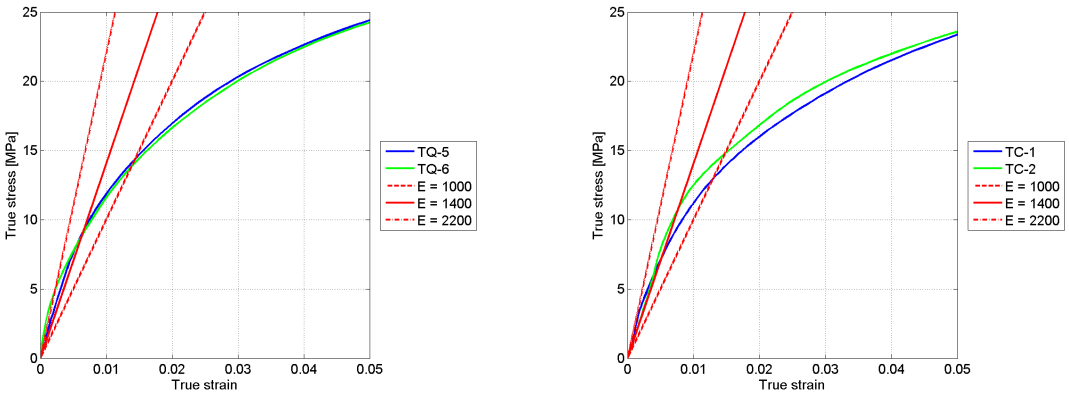

(a) TQ

(b) TC

Figure 5.3: Young's modulus for HDPE

Figure 5.4 shows a plot of Poisson's ratio for the HDPE TQ tests. The circular tests suggest a lower Poisson's ratio than the quadratic tests, but neither geometry

gives a constant value in the elastic domain. A value of 0.43 has been chosen for the numerical simulations.

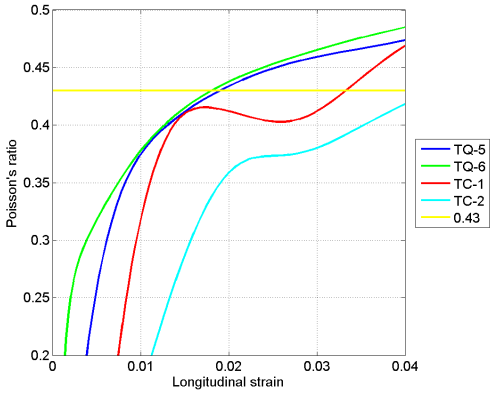

Figure 5.4: Poisson's ratio for HDPE

After determining the Young's modulus E, the tension yield stress σ_T can be determined. Assuming yielding at 0.2% plastic strain for materials with hardening, as described in Section 5.1, gives the plot in Figure 5.5(a). Observing where the line crosses the stress-strain curves, a yield stress of $\sigma_T = 12.1$ MPa is chosen.

Performing the same procedure for the compression tests, the yield stress in compression is found to be equal to that in tension. This can be seen in Figure 5.5(b). Using Equation (2.14) with equal values of σ_C and σ_T, gives $\alpha = 1$.

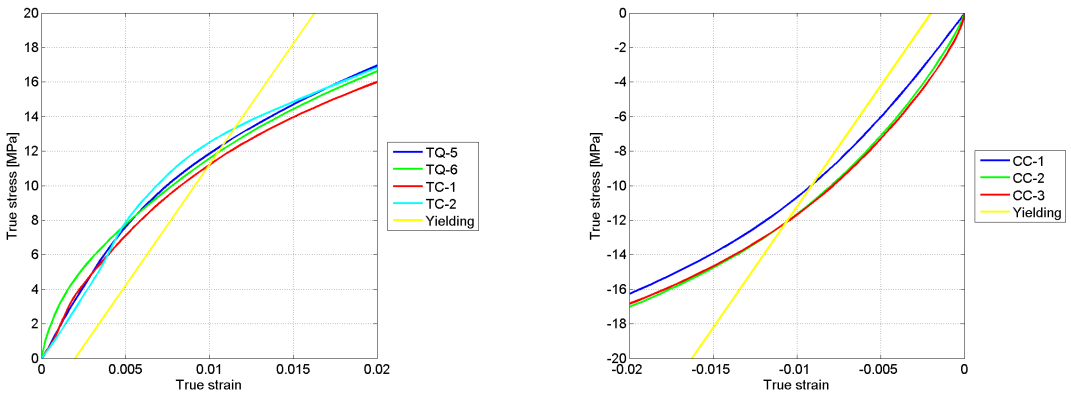

(a) Determining σ_T

(b) Determining σ_C

Figure 5.5: Yield stresses in tension and compression for HDPE

In order to determine σ_S for HDPE, Considère's criterion has been used. Figure 5.6(a)

shows the criterion from Equation (5.19) plotted against the stress for test TQ-5. The stress value where this line crosses the x-axis is used as the saturation stress. This corresponds to the stress value where the tangent of the stress-stretch curve intersects the origin, as shown in Figure 5.6(b). Based on all the tests, the saturation stress is determined to be $\sigma_S = 28.6$.

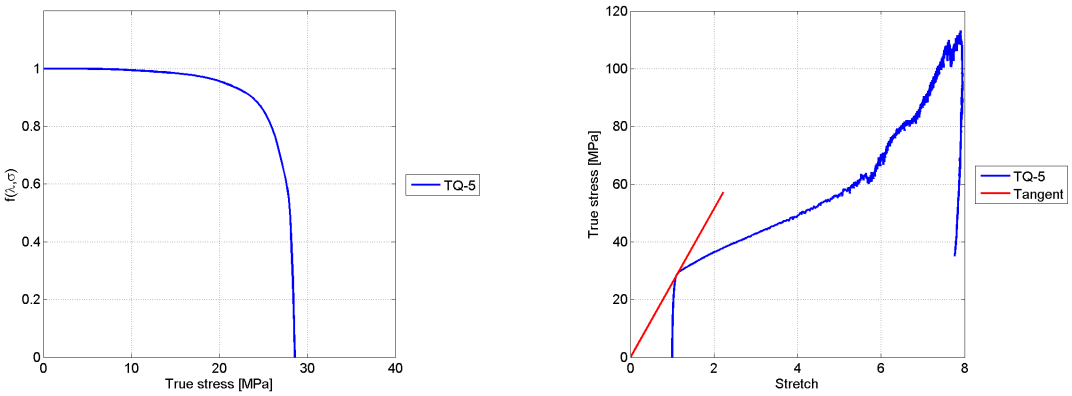

(a) Considère's criterion

(b) True stress plotted against stretch

Figure 5.6: Determining σ_S using Considère's criterion

The ramping parameter H is calculated using Equation (5.22). For HDPE, a target plastic strain of $\varepsilon^p_{A,S} = 0.053$ has been used, resulting in $H = 56$.

The plastic volumetric strain parameter β can be found by determining the contraction ratio ρ in the plastic domain, see Equation (5.3). This ratio is plotted in Figure 5.7 for the tension tests; the results differ for the two geometries, so an average of $\rho = 0.44$ is chosen. Using Equation (5.18), this gives $\beta = 1.08$.

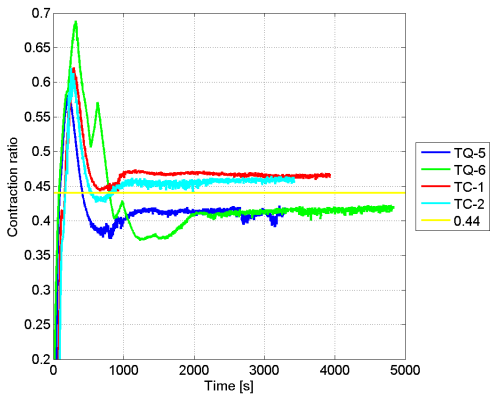

Figure 5.7: Contraction ratio of HDPE tests

5.3.2 Part B

The value for C_R was obtained from a previous specialization project about HDPE performed by Røstum and Winjum [9]. There, a value of $C_R = 1.63$ had been found for the initial stiffness of the part B spring.

Using the experimental results, a rough estimate of the locking strain ε_L was chosen as 2.3 and used in Equation (5.29). Thus, the locking stretch was determined to be $\bar{\lambda}_L = 5.26$.

5.3.3 Summary

After performing numerical simulations with the parameter values obtained in this section, some parameters were adjusted to give a better fit between the results from the experiments and the simulations. For HDPE, only C_R, $\bar{\lambda}_L$, σ_S and H were adjusted slightly, and the final values used in the simulations are presented in Table 5.1.

Table 5.1: Parameters for HDPE

E	ν	$\dot{\varepsilon}_{0A}$	$C(\theta)$	σ_T	C_R	$\bar{\lambda}_L$	α
1400	0.43	10^{-2}	0.12	12.1	1.5	5.6	1.00
β		σ_S	H			K	G
1.07		26.1	56			3333	490

5.4 Calibration of PVC

5.4.1 Part A

Also for PVC, the first parameter to be determined is Young's modulus E. Figure 5.8 shows the stress-strain curves for both the quadratic and cylindrical geometries, with examples of different values of E. A value of 2800 MPa is chosen, as this follows the curves very closely in the elastic domain.

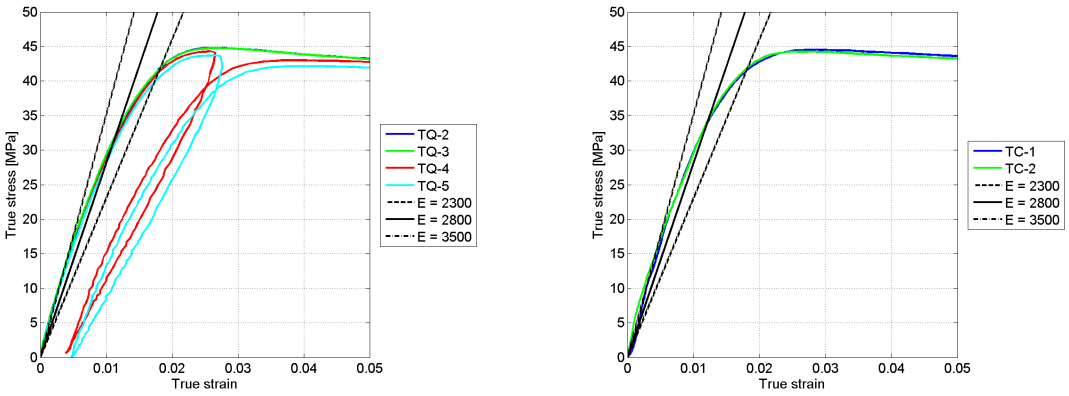

(a) TQ (b) TC

Figure 5.8: Young's modulus for PVC

As with HDPE, the TC tests show a slightly lower Poisson's ratio than the TQ tests in Figure 5.9. A value of $\nu = 0.38$ seems to be a good fit and is chosen for the numerical simulations of PVC.

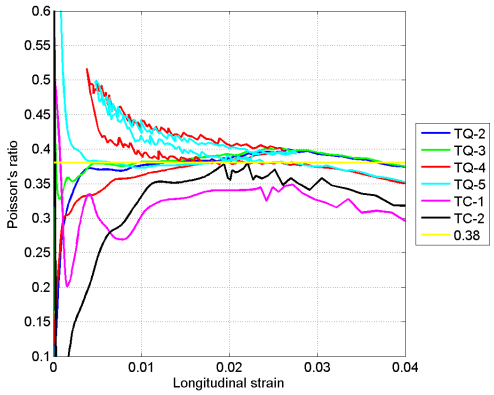

Figure 5.9: Poisson's ratio for PVC

As explained in Section 5.1, a different method for determining σ_T, σ_S and σ_C is used for materials with softening after yielding. These values are found from the local maximums and minimums of the stress-strain curves. Figure 5.10(a) shows how σ_T and σ_S were determined for test TQ-3, while Figure 5.10(b) shows how σ_C was determined for test CC-1.

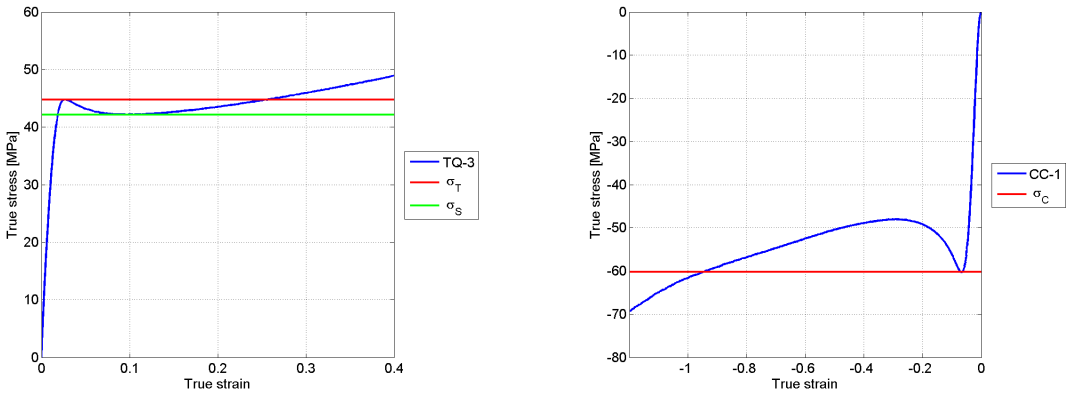

(a) σ_T and σ_S of TQ-3

(b) σ_C of CC-1

Figure 5.10: Determining σ_T, σ_S and σ_C of PVC

After the results of all the PVC tests were processed, the following values were obtained: The tensile yield stress is $\sigma_T = 44.4$ MPa, the yield stress in compression is $\sigma_C = 59.0$ MPa, and the saturation stress was found to be $\sigma_S = 42$ MPa. The parameter α can then be calculated:

$$\alpha = \frac{\sigma_C}{\sigma_T} = \frac{59.0}{44.4} = 1.33 \tag{5.30}$$

For PVC, the target plastic strain $\varepsilon^p_{A,S}$ was set to 0.13. Using Equation (5.22), this results in a ramping parameter of $H = 23$.

Figure 5.11 shows a highly nonlinear behavior of the contraction ratio ρ in the plastic domain for PVC. It is therefore hard to determine an accurate constant value of ρ for this material, but 0.39 has been chosen in this thesis. The parameter β in the plastic potential function is then determined to be equal to 1.16, using Equation (5.18).

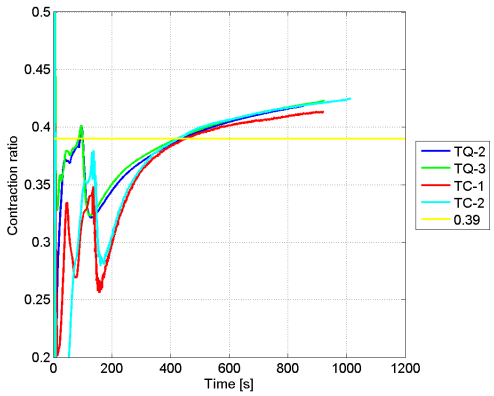

Figure 5.11: Caption for PVC-rho

5.4.2 Part B

Results from Hovden's work [4] was used to set a value for the initial stiffness C_R of the spring in part B, where this was determined to be equal to 6.07. From the experimental results, an estimated locking strain of 1.41 was chosen. Using Equation (5.29), the locking stretch was determined to be $\bar{\lambda}_L = 2.27$.

5.4.3 Summary

All the parameters used in the material model for PVC are listed in Table 5.2. After the initial calibration, the parameters σ_T, C_R, σ_S and H have been adjusted using inverse modeling.

Table 5.2: Parameters for PVC

E	ν	$\dot{\varepsilon}_{0A}$	$C(\theta)$	σ_T	C_r	λ	α
2800	0.38	1^{-3}	0.07	46.5	8.0	2.27	1.33
β		σ_S	H			K	G
1.16		33.0	15			3889	1015

Chapter 6

Numerical simulations

This chapter will present the numerical simulations that were performed using the parameters obtained in Chapter 5. All the simulations were performed in the finite element method (FEM) program LS-DYNA. The first section gives a description of how the different geometries were modeled. Then, there is one section on the simulation of each material, detailing how the simulations compare to the experimental results.

6.1 Model geometries

Because of the curved surfaces of the specimens, they are hard to draw and mesh in LS-DYNA. Another FEM program, Abaqus, was therefore used to draw and mesh the geometries of the specimens. Since the material model was only available for LS-DYNA, the mesh from the Abaqus input file had to be converted to an LS-DYNA k-file using Matlab.

Since all the geometries have two symmetry planes along its center line, only one quarter of the specimens have been modeled. This reduces the number of elements in the model, and greatly decreases the computation time. Boundary conditions are then applied in order to make the specimen behave correctly.

6.1.1 Tension geometries

Figure 6.1 and 6.2 show the TQ and TC geometries respectively. During the experimental tests, about half the length of the specimens' handles were clamped in the test machine. Only 15 mm of the total 30 mm handles were therefore modeled. In the simulations, one end of the specimen has held in place by boundary conditions, while the other end was subjected to a prescribed displacement equal to that of the experiments.

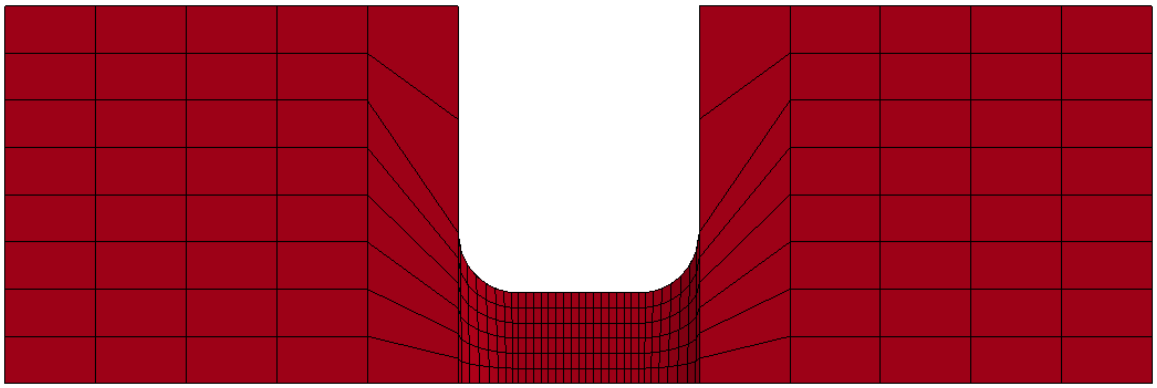

(a) Front

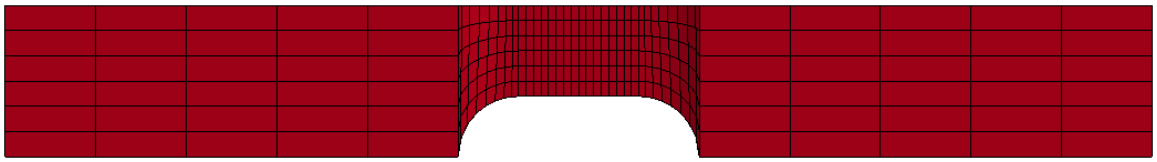

(b) Top

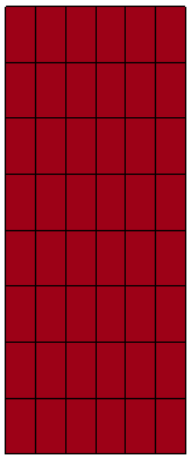

(c) End

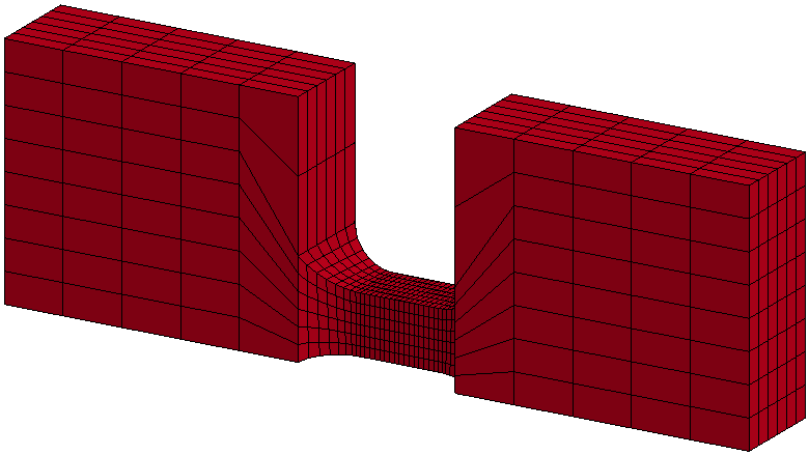

(d) 3D view

Figure 6.1: TQ geometry in LS-DYNA

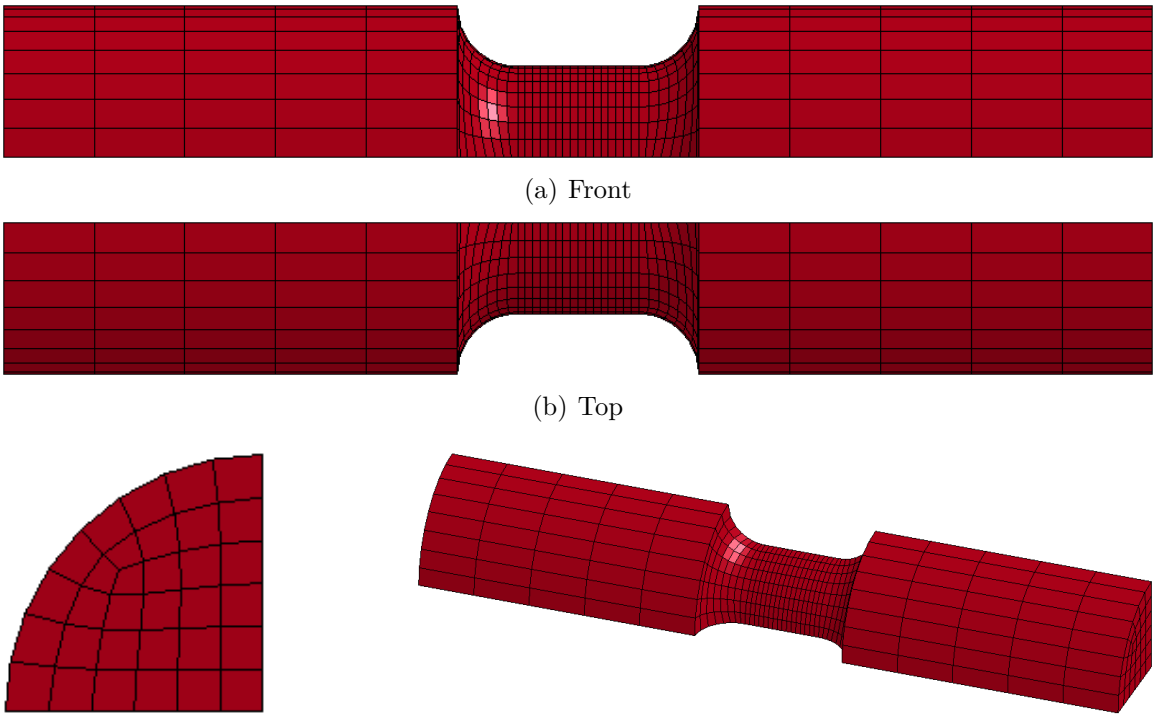

(a) Front

(b) Top

(c) End

(d) 3D view

Figure 6.2: TC geometry in LS-DYNA

6.1.2 Compression geometry

The CC geometry is shown in Figure 6.3. Because of the friction between the test machine's surface and the specimen, a displacement cannot simply be applied to the top of the specimen. In order to account for the friction in the model, two boxes have to be included above and below the specimen. The box above the specimen is then applied the displacement, and a friction coefficient determines the behavior in the contact surfaces between the specimen and boxes.

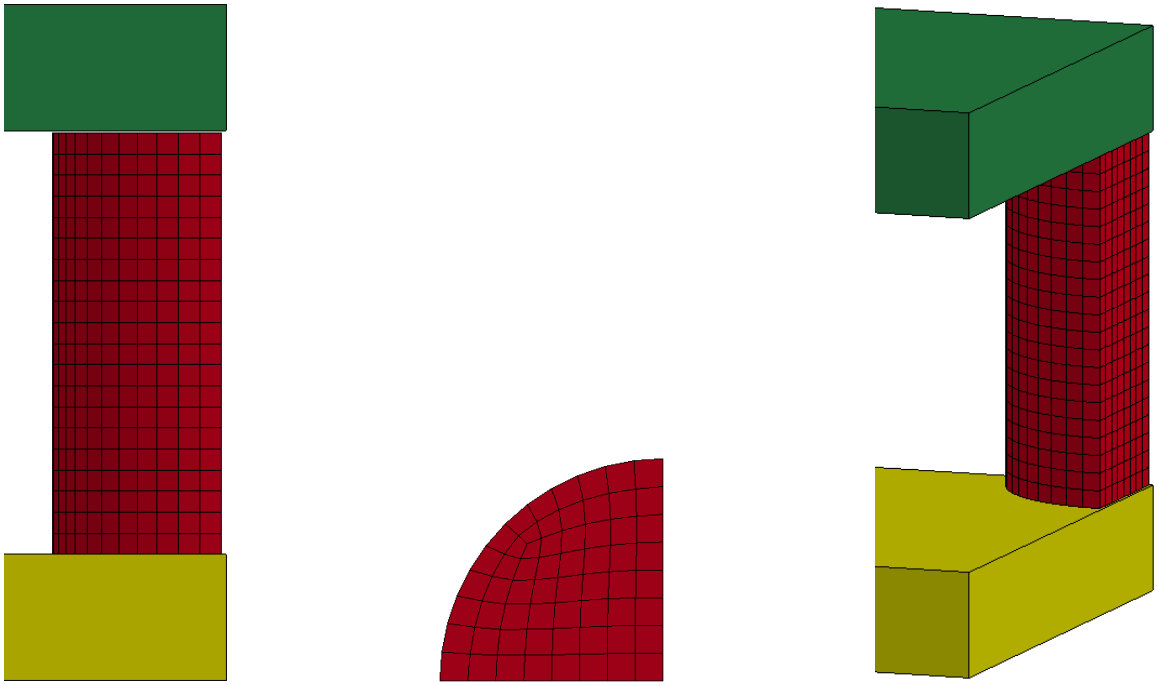

(a) Front (b) Top (c) 3D view

Figure 6.3: CC geometry in LS-DYNA

6.2 HDPE

The following results are based on simulations using the parameters from Table 5.1.

6.2.1 Tension tests

Stress-strain

As the stress-strain curves are the primary basis of the calibration, these results will be presented first. After a numerical analysis has been performed in LS-DYNA, the strains and stresses of each element can be gathered from the output files of the program. Previous studies[10][9] on this material model have used the elements in the section where necking first start when presenting the results of the simulations. Figure 6.5(a) and (b) shows these elements for the TQ and TC geometry, respectively. The resulting stress-strain curves of these elements are compared to the experimental tests in Figure 6.5(c). This method of obtaining the strains and stresses from the simulations will be referred to as the element method in the rest of this thesis.

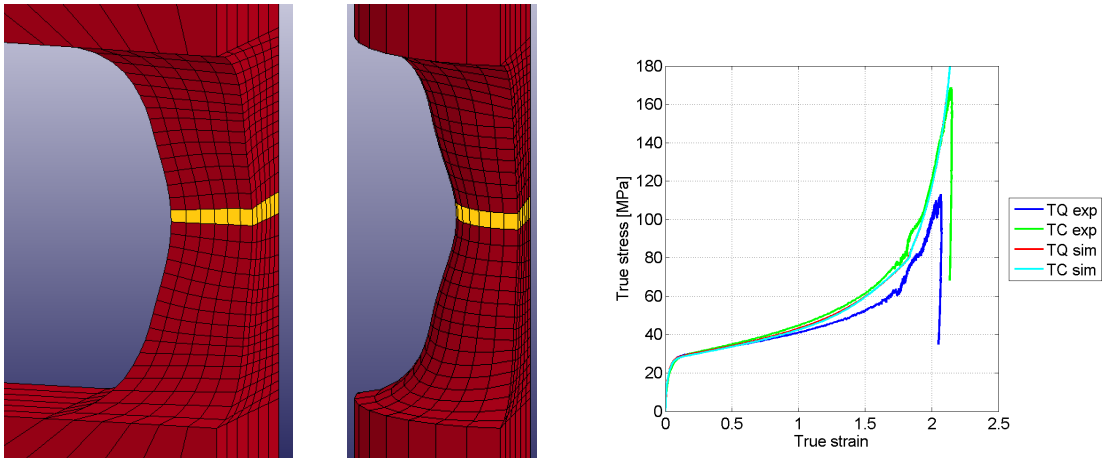

(a) TQ (b) TC (c) Stress-strain curves

Figure 6.4: Stress-strain curves using the element method

As opposed to the experimental results, the results from the simulations show almost no difference between the two geometries. This seems more logical, as a given material should have the same stress-strain relation independent of the specimen geometry. The reason for the difference in the experimental results become apparent when using a different method of obtaining the strains and stresses, which will be referred to as the node method. Using only the relative displacements of the nodes on the surface of the specimens, the strains can be calculated by

$$\varepsilon = \ln \frac{L}{L_0} \tag{6.1}$$

This is the same way the strains are obtained from the DIC analysis, and should match the experimental results better. The stresses are calculated by determining the cross-section area from the transverse strains, and dividing the force from the simulation by this area. This is the same procedure as used for the experimental results in Section 3.3. Figure 6.5(a) and (b) shows the nodes that were used, and Figure 6.5(c) compares the stress-strain curves of the experimental tests and the node method. This method gives a perfect match for both geometries.

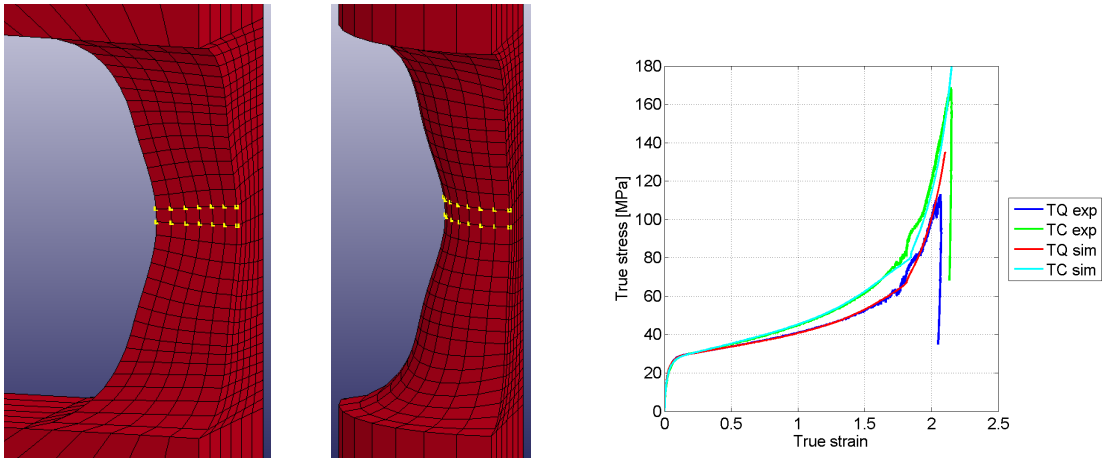

(a) TQ (b) TC (c) Stress-strain curves

Figure 6.5: Stress-strain curves using the node method

Even though the node method gives a better match of the experimental results, the element method may give a better representation of the actual material behavior. In the experimental results, it is only possible to study the surface of the specimens, and this might not give an accurate picture of what happens inside. Given the perfect match of the surface behavior using the node method, it can be assumed that the element method accurately represents the material behavior inside the test specimens. A material should have the same response regardless of the shape of the specimen, and this is achieved by the element method.

Strain rate

The stress-strain curve is a perfect match when using the node method, but Figure 6.6(a) shows that the strain increases a lot faster in the simulations than the experiments. The fact that the stress also increases faster in the simulations, as seen in Figure 6.6(b), is why the stress-strain curve still matches. Only the TQ results are shown here, as the TC results are very similar.

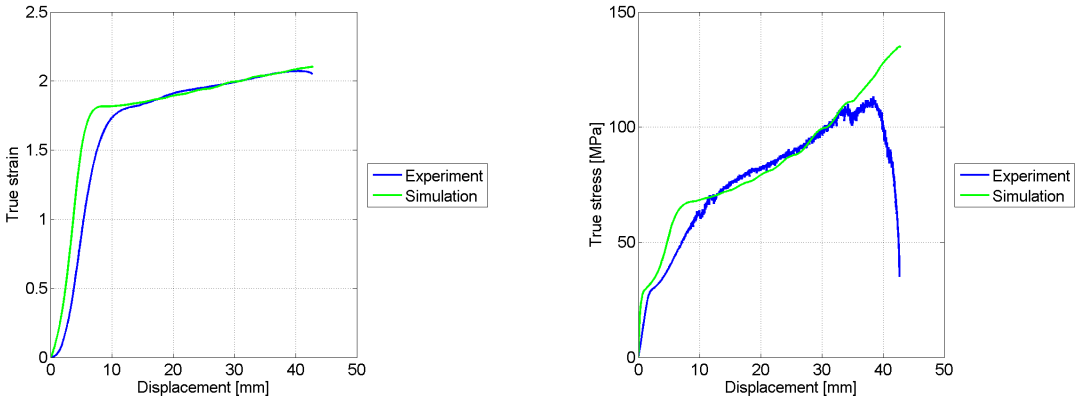

(a) Strain-displacement

(b) Stress-displacement

Figure 6.6: Comparing strains and stresses between experiments and simulations for TQ using the node method

Figure 6.7(a) clearly shows how the simulations have a much higher strain rate at the start of the tests. This can also be observed by comparing the pictures taken during the test with the simulation, as in Figure 6.7(b). In the simulations, the deformation is focused on the elements in the middle of the gauge area, and the neck does not spread to the other elements until the middle ones have nearly reached locking. The experimental tests have a more diffuse necking, and the strains are distributed more uniformly along the gauge area.

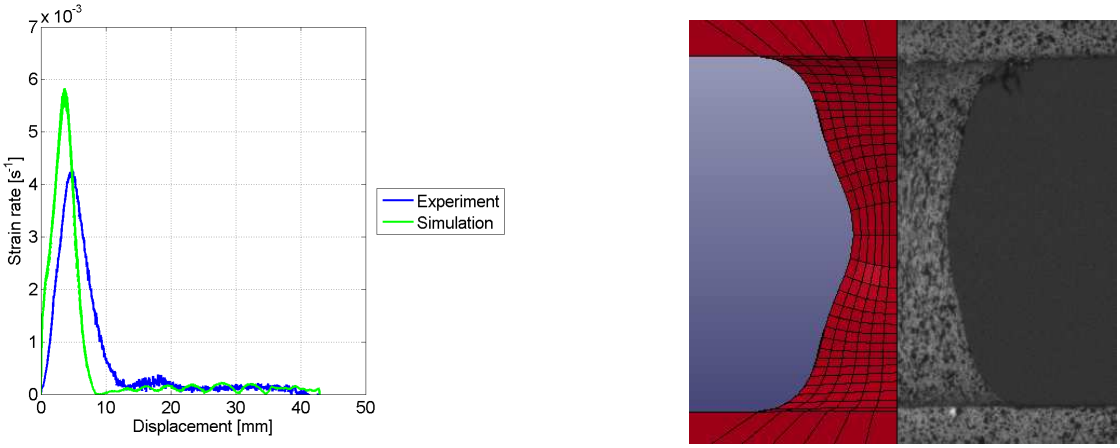

(a) Strain rate

(b) Simulation and experimental test at 5 mm displacement

Figure 6.7: Strain rate

Force-displacement

Figure 6.8 shows the force-displacement curves of the HDPE tension simulations. The slope of the curve from the simulations are steeper than those of the experimental test. This could be caused by the model being too stiff, but since the stress-strain curve fit very well, this is most likely not the case. It can be explained by the higher strain rate in the simulations. Figure 6.6 shows that yielding is reached at a smaller displacement in the simulations.

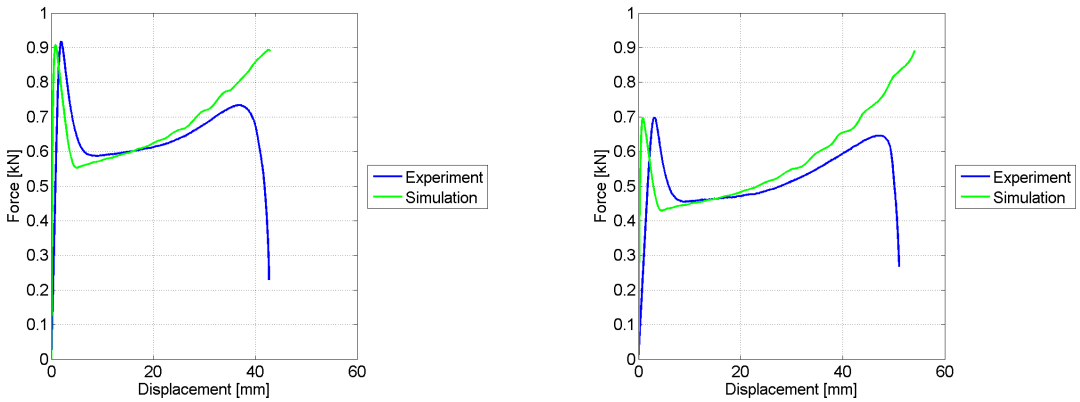

(a) TQ (b) TC

Figure 6.8: Force-displacement curves

Volumetric strain

The results from the experimental tests showed a negative volumetric strain in the tensile HDPE tests. Using the node method for obtaining the strains, these results were reproduced in the simulations, as illustrated in Figure 6.9.

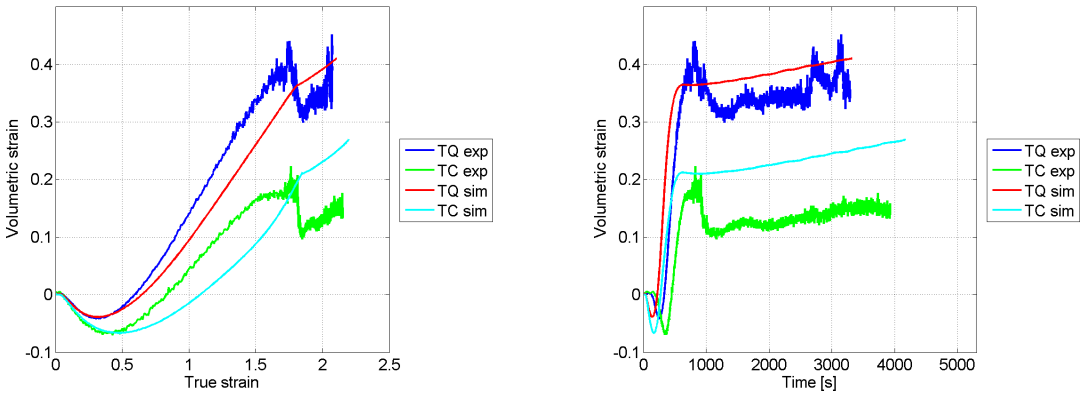

(a) Volumetric vs. longitudinal strain (b) Volumetric strain vs. time

Figure 6.9: Volumetric strains using the node method

Since this material should not be able to have negative volumetric strain in tension, it is likely that the element method gives a better description of the actual material behavior; these results are presented in Figure 6.10.

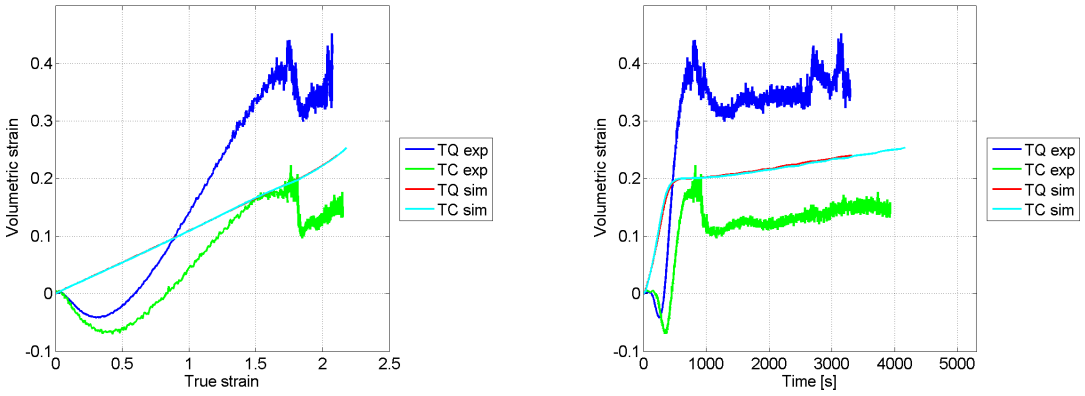

(a) Volumetric vs. longitudinal strain (b) Volumetric strain vs. time

Figure 6.10: Volumetric strains using the element method

A comparison of the longitudinal, transverse and volumetric strains in the elastic domain from both methods is shown in Figure 6.11. The negative volumetric strains from the node method are caused by the difference in longitudinal strain, as the transverse strains are fairly equal in this region. For both geometries, the longitudinal strain eventually ends up at the same value. Only the TC geometry ends up with an equal transverse strain. The TQ geometry ends up with higher transverse strains when using the element method, and therefore a lower volumetric strain.

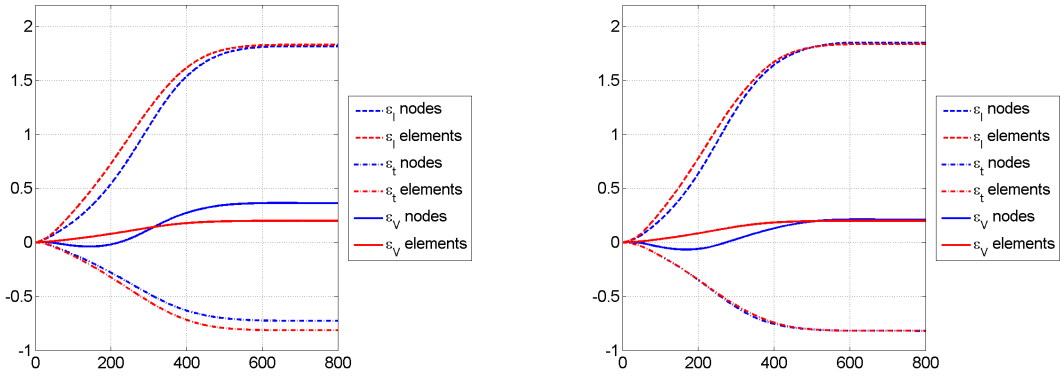

(a) TQ

(b) TC

Figure 6.11: Comparison of longitudinal, transverse and volumetric strains

The reason for the difference in longitudinal strains between the two methods can be seen from Figures 6.12 and 6.13. For the TQ geometry in Figure 6.12(a), three pairs of nodes were selected, one in the center, one on the side, and one on the corner of the specimen. The different strain rates in these three areas are plotted in Figure 6.12(b).

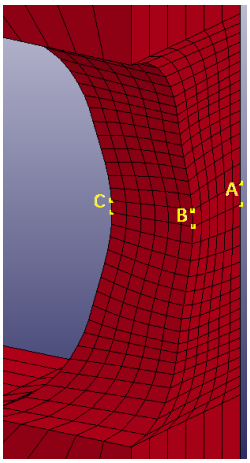

(a) A: Center. B: Side. C: Corner

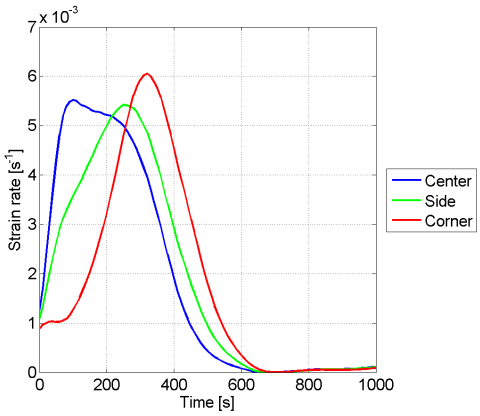

(b) Strain rates

Figure 6.12: Strain rates for HDPE TQ

For the TC geometry, two pairs of nodes were selected as illustrated in 6.13(a), and the resulting strain rates are shown in Figure 6.12(b).

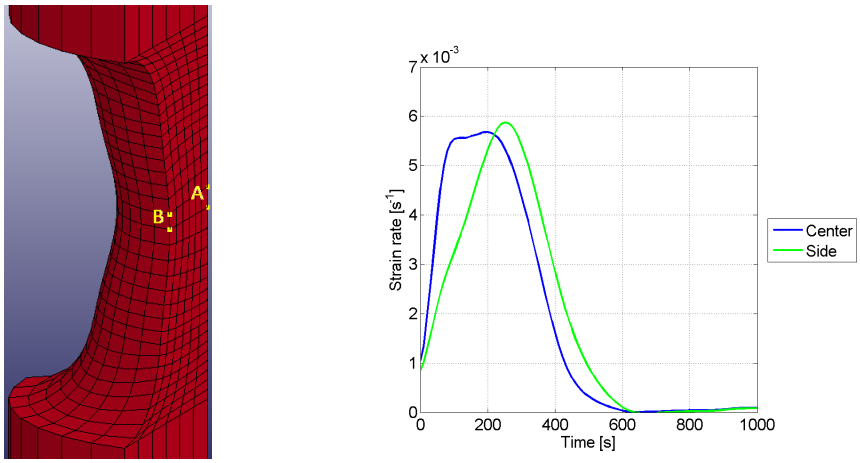

(a) A: Center. B: Side

(b) Strain rates

Figure 6.13: Strain rates for HDPE TC

For both geometries, the center of the specimen has a much higher longitudinal strain rate at the start of the test. The strain at the surface catches up later on, but this delay gives the impression of a negative volumetric strain when observing the surface of the specimen.

Cyclic loading

A cyclically loaded test based on the displacement history of HDPE TQ test 6 was simulated. The resulting force-displacement and stress strain curves are given in Figure 6.14. These results does not give a very good match. The higher strain rate in the start of the simulations shifts the cycles towards the end of the stress-strain curve. Using the displacements that unloaded the experiments to zero force actually gives the simulations a negative force at small strains, but does not even reach zero force for larger strains.

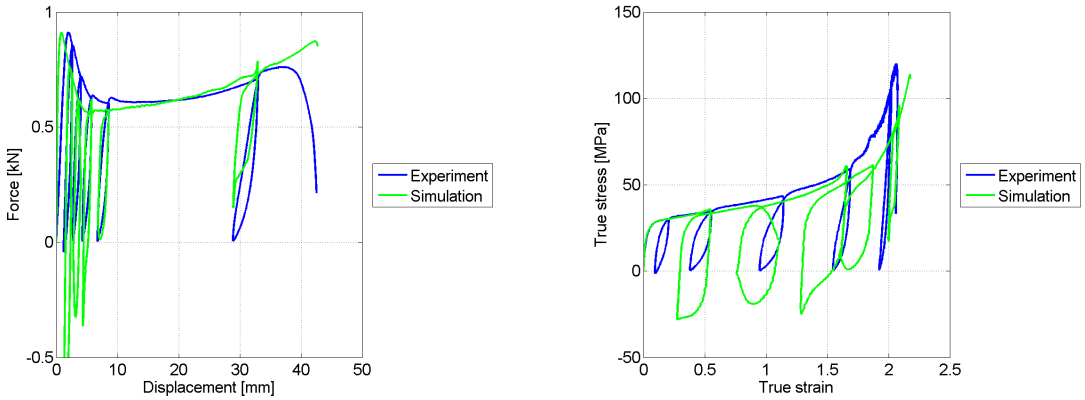

(a) Force-displacement

(b) Stress-strain

Figure 6.14: Caption for HDPEsimcycl-FD

6.2.2 Compression tests

Stress-strain

Since the material model was calibrated based on the tension tests, the results of the compression simulations can not be expected to be as accurate as the tension simulations. Figure 6.15 shows the results from the simulations using the element method for obtaining the strains. Although the curves do not follow each other as close as those of the tensile tests, the results are quite good. As explained in Chapter 4, the DIC analysis did not give an accurate result for the longitudinal strains. Since the node method of the simulations is equivalent to the DIC analysis, these results have been compared in Figure 6.15(b). The value at which the strains stops is highly dependent on the friction coefficient used in the simulation. For these simulation this coefficient has been set to 0.06. For the tensile tests, there was no good way to compare the experimental tests to the element method; with the compression tests there is, using the strains based on displacement from the experiments. The good match in both node and element method suggests that the element method can represent the whole material accurately when the node method matches the surface behavior.

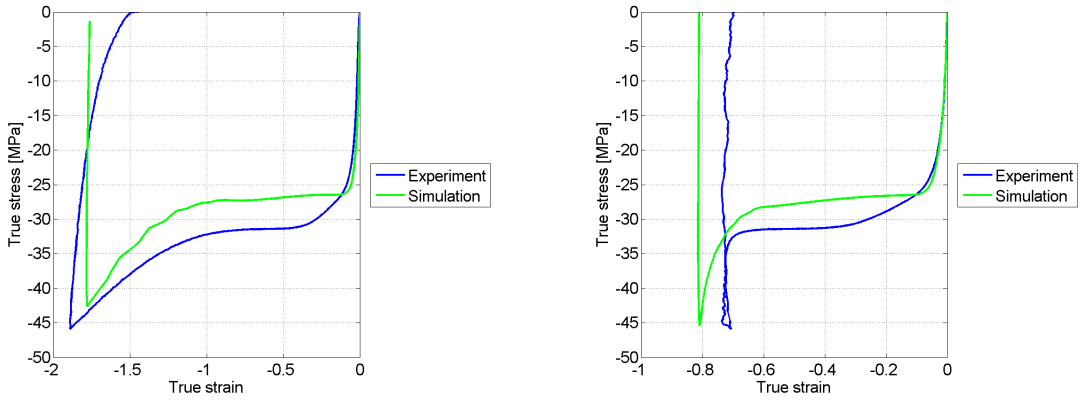

(a) Element method (b) Node method

Figure 6.15: Force-displacement curves

Force-displacement

Figure 6.16(a) shows the force-displacement curve of the HDPE compression test simulation. Compared to the experimental tests, this reaches a much higher maximum force. This error is due to the specimen's cross section area increasing a lot more in the simulation, as seen in Figure 6.16(b). The simulations are only based on the displacement history of the experimental tests, and when the material expands to a larger cross section area, a higher force is required.

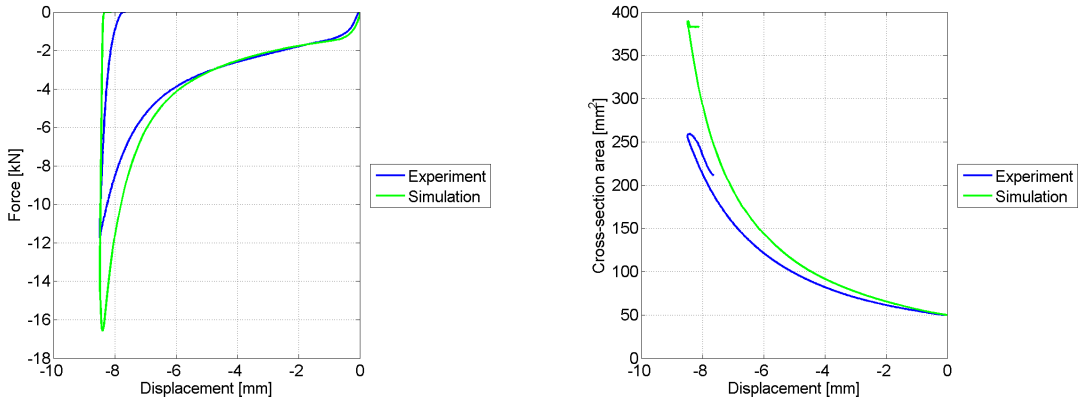

(a) Force-displacement (b) Cross section area

Figure 6.16: HDPE compression tests

Volumetric strain

Figure 6.17 compares the longitudinal, area and volumetric strains of both the experiment and simulation. The larger area strains of the simulations leads to positive volumetric strains in compression.

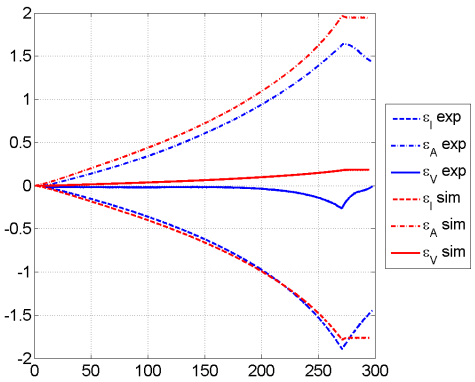

Figure 6.17: Longitudinal, area and volumetric strains for HDPE compression experiment and simulation

6.3 PVC

The parameters from Table 5.2 were used to simulate the material behavior of PVC.

6.3.1 Tension tests

Stress-strain

Figure 6.18 shows a comparison of the stress-strain relation from the PVC tension experiments and simulations. Both the node and the element method is presented, and the difference between these is smaller than for HDPE. The only difference is a higher yield stress when using the element method.

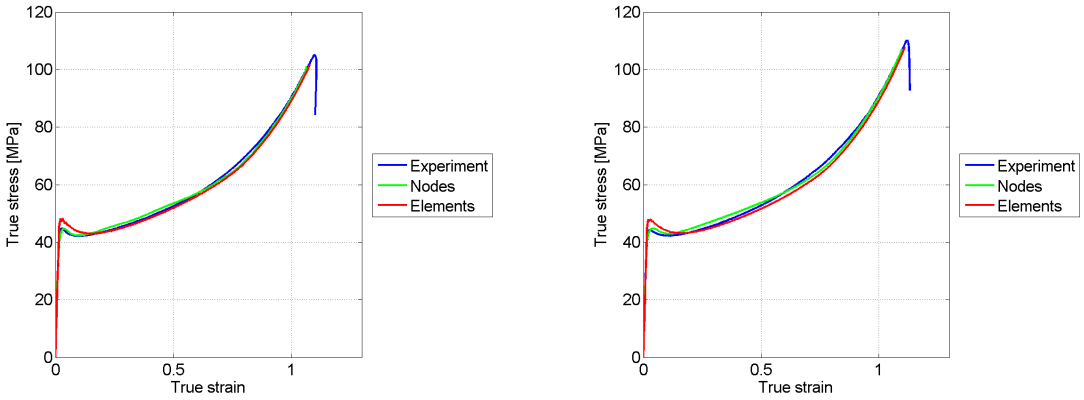

(a) TQ (b) TC

Figure 6.18: Stress-strain curves for PVC tension simulations using both node and element method

Strain rate

The difference in strain rate at the start of the test between the experiment and simulation is even more apparent for PVC than it was for HDPE. Figure 6.19 gives the strain and stress from the PVC TC test plotted against displacement. Similar results are found for the TQ geometry.

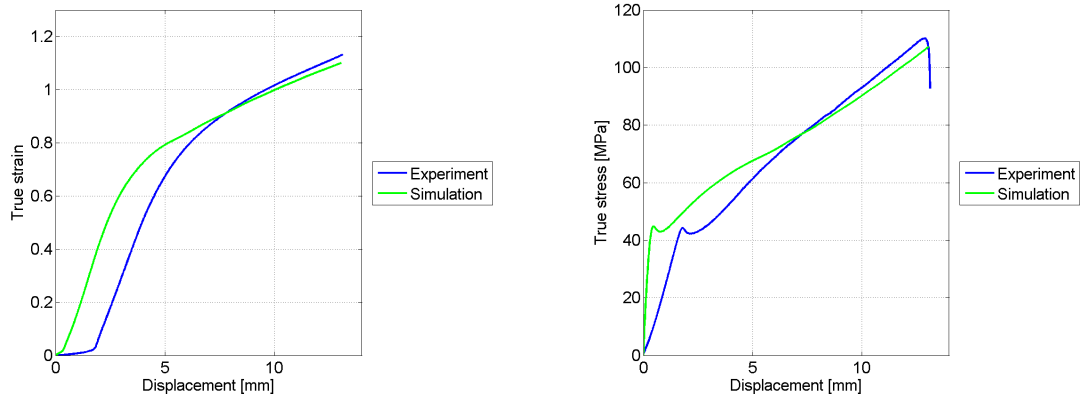

(a) Strain-displacement (b) Stress-displacement

Figure 6.19: Comparing strains and stresses between experiments and simulations for TC using the node method

The strain rate for PVC is given in Figure 6.20(a) and shows a large difference in the timing of the maximum strain rate. An image comparing the geometry at 1 mm

displacement is shown in Figure 6.20(b). The simulation has started showing signs of necking at this point, while the experimental test specimens still has a straight gauge section.

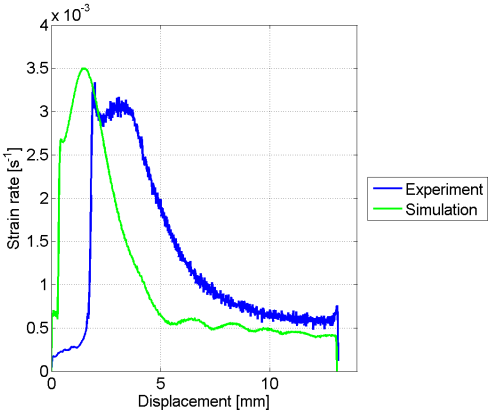

(a) Strain rate

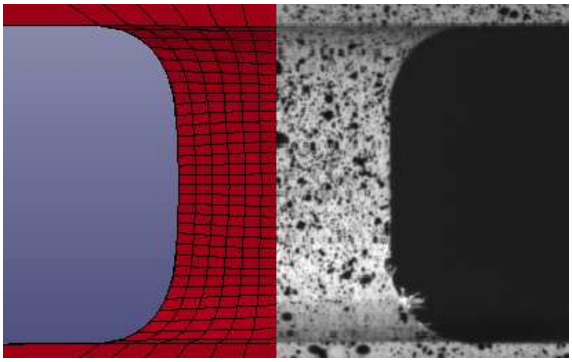

(b) Simulation and experimental test at 1 mm displacement

Figure 6.20: Strain rate

Force-displacement

Again, the force-displacement curves from the simulations are off due to the difference in strain rate. The discrepancy is even larger for PVC than for HDPE.

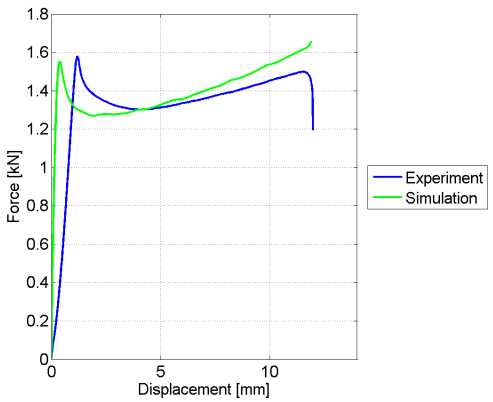

(a) Volumetric vs. longitudinal strain

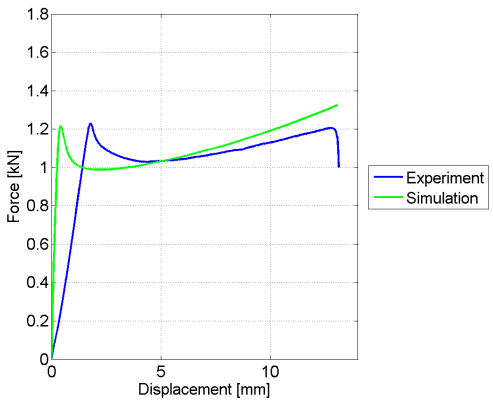

(b) Volumetric strain vs. time

Figure 6.21: Force-displacement curves for PVC TQ simulations

Volumetric strain

The volumetric strains of the PVC tension tests are presented in Figure 6.22 and 6.23. In this case, the node method actually does not give a good match. The simulations give a negative volumetric strain at the start of the test, which was not the case for the experiments. This is due to the significant necking of the simulations, while the PVC experiments actually had a very diffuse necking. This problem with reproducing the volumetric strain results could be due to void growth in the specimens, something the numerical model is not able to account for.

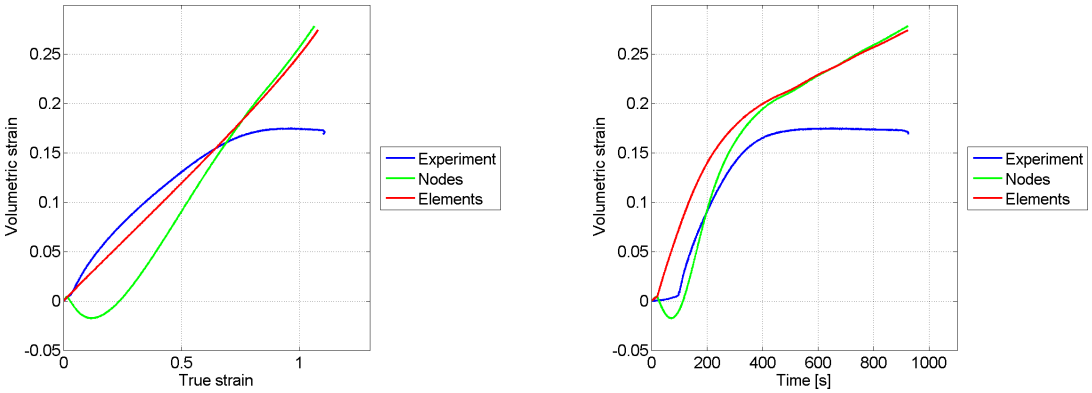

(a) Volumetric vs. longitudinal strain (b) Volumetric strain vs. time

Figure 6.22: Volumetric strain curves for PVC TQ simulations

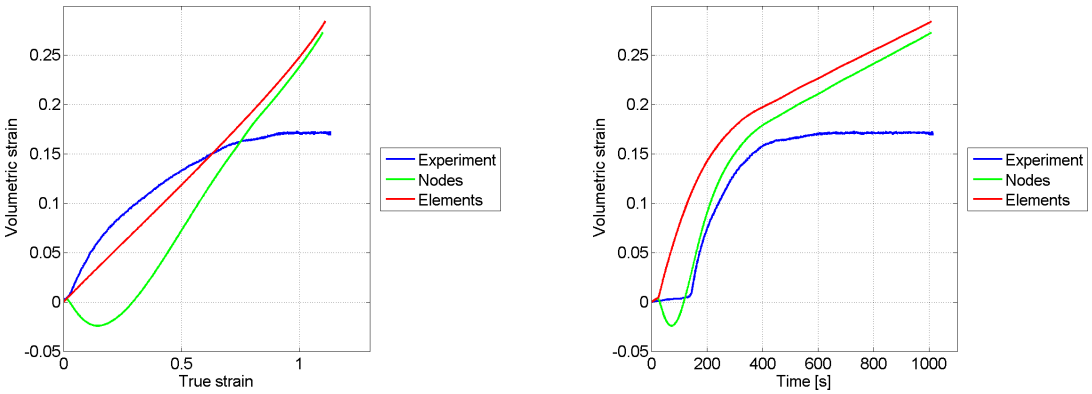

(a) Volumetric vs. longitudinal strain (b) Volumetric strain vs. time

Figure 6.23: Volumetric strain curves for PVC TC simulations

Cyclic loading

From Figure 6.24 it can be seen that the same problems arises for PVC when simulating cyclic loading. The unloading cycles result in negative forces for the simulations, and the cycles are shifted towards the end of the stress-strain curve.

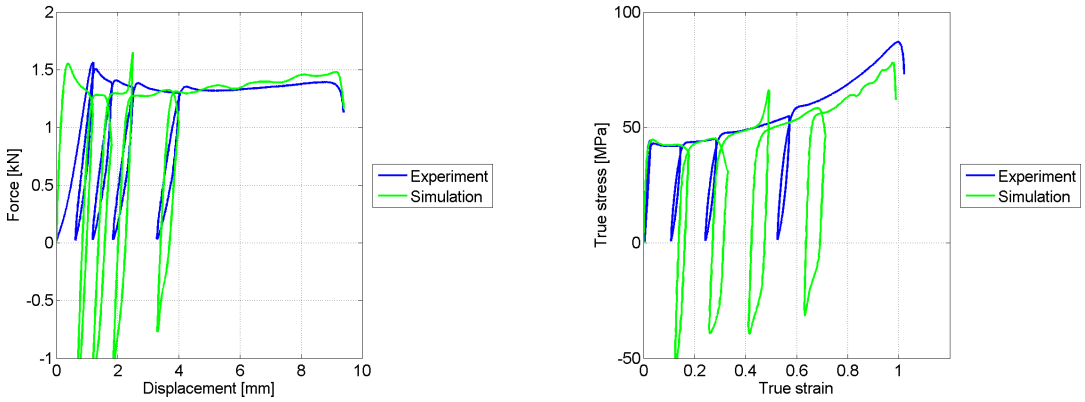

(a) Force-displacement

(b) Stress-strain

Figure 6.24: Cyclically loaded simulation

6.3.2 Compression tests

Stress-strain

The PVC compression simulations show a much higher stress than the simulations in Figure 6.25; this suggests a much larger force in the simulations. The node method gives a good comparison to the DIC strains in Figure 6.25(b), using a friction coefficient of 0.06 also for PVC.

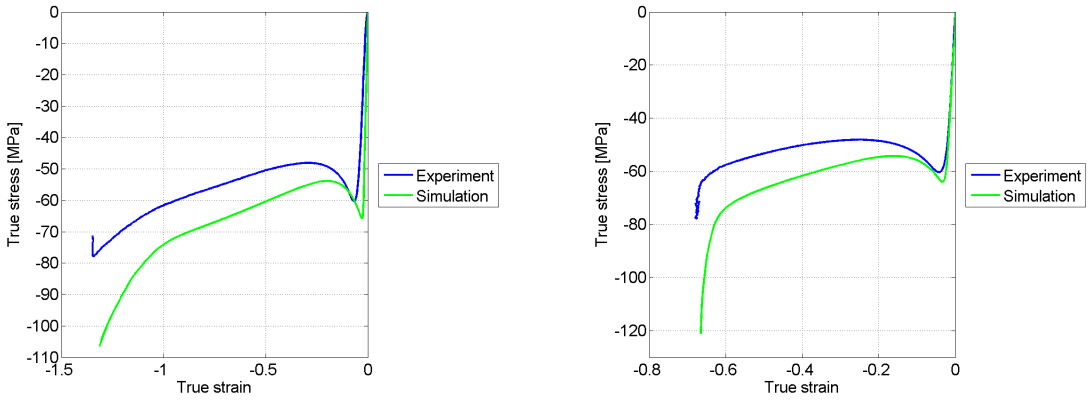

(a) Element method (b) Node method

Figure 6.25: Force-displacement curves

Force-displacement

As expected from the stress-strain curve, the force is larger in the simulations than the experiments, as seen in Figure 6.26. As for HDPE, this is due to the cross section area becoming larger and increasing the resistance of the specimen. This can be seen in Figure 6.26(b).

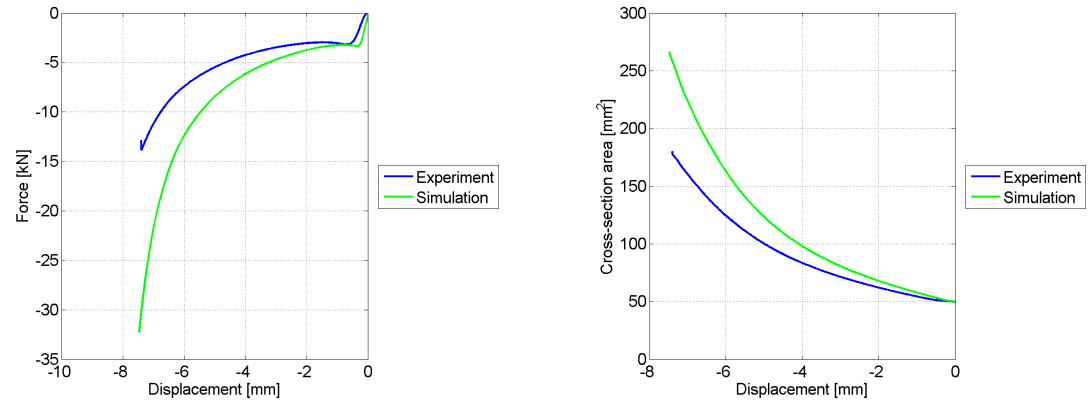

(a) Element method (b) Node method

Figure 6.26: Force-displacement and cross section area

Volumetric strain

Just like with HDPE, the area strain is larger in the simulations and gives a positive volumetric strain for the compression tests; this is illustrated in Figure 6.27.

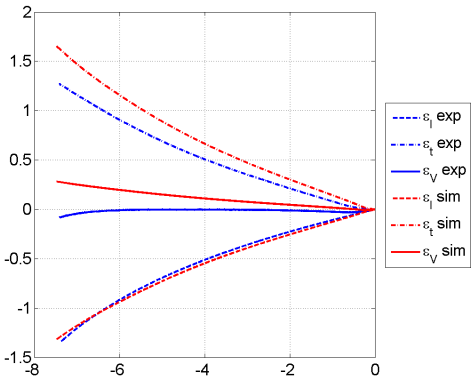

Figure 6.27: Volumetric strain for PVC compression tests

Chapter 7

Conclusion

Overall, the material model is able to reproduce the experimental tests very well. Both the stress-strain and force-displacement relations from the numerical simulations give a close match to those of the experimental tests. There are, however, certain problems with reproducing the correct strain history. In the simulations, necking occurs earlier and is more pronounced than in the experimental results. Almost all the deformation in the early stages of the simulation is focused on the elements in the section where necking first starts. There is almost no propagation of the neck until these elements have reached locking stretch. The experimental tests show a more diffuse necking, and the deformations are more evenly distributed along the gauge area at the early stages of the tests. For the compression geometry, there was a problem of too much expansion of the material in the transverse direction in the simulations. This resulted in the cross-section area, and in turn the force, being too large; it also gave a positive volumetric strain in compression.

In this thesis, two methods of determining the strains of the numerical simulations have been suggested. One uses the strains directly from the elements, while the other uses the relative displacement of the nodes on the surface of the specimen to calculate the strains. The node method is equivalent to the way strains from the experimental tests are determined using DIC, so this method is great for comparison between experiments and simulations. As this method only observe the surface of the specimen, this could lead to some small errors in the results. The strains from the element method should therefore be assumed to give the correct representation of the material behavior. The difference between the two methods may seem insignificant when evaluating the stress-strain relation; but other results, like the volumetric strain, is very sensitive to which method is used.

A new tension geometry, with a circular cross-section, was tested in this study. The results from this geometry were overall better than those from the quadratic geometry. The corners of the quadratic geometry give a strain field that varies along the specimen's surface. This problem is completely eliminated by using a circular geometry. Also, the difference between the two methods of determining the strains of the simulations is smaller for the circular geometry. This suggests that the difference in strain rate between the center of the specimen and the surface is also smaller using this geometry. It is therefore recommended that the circular geometry is used for future experiments.

Suggestions for further work

The reason behind the high strain rate at the start of the simulations should be looked more into. A solution to this would greatly improve the accuracy of the numerical simulations.

Due to time constraints, the cyclically loaded tests were not given much attention in this thesis. The simulations of these tests did not produce accurate results, and should be studied further.

Bibliography

[1] Arie Ram. *Fundamentals of polymer engineering*. Plenum Press, 1997.

[2] Joachim Rösler, Harald Harders, and Martin Bäker. *Mechanical Behaviour of Engineering Materials*. Springer, 2007.

[3] Mario Polanco-Loria, Arild H. Clausen, Torodd Berstad, and Odd Sture Hopperstad. Constitutive model for thermoplastics with structural applications. *International Journal of Impact Engineering*, (37):1207–1219, 2010.

[4] Martin Thuve Hovden. Tests and numerical simulations of polymer components. Master's thesis, Norwegian University of Science and Technology, NTNU, 2010.

[5] Odd Sture Hopperstad and Tore Børvik. *Lecture Notes, Material Mechanics*. NTNU, Structual Impact Laboratory, 2013.

[6] Ram Raghava, Robert M. Caddell, and Gregory S. Y. Yeh. The macroscopic yield behaviour of polymers. *Journals of Materials Sience*, (8):225–232, 1973.

[7] Anne Serine Ognedal, Arild Holm Clausen, Mario Polanco-Loria, Ahmed Benallal, Bumedijen Raka, and Odd Sture Hopperstad. Experimental and numerical study on the behaviour of pvc and hdpe in biaxial tension. *Mechanics of Materials*, (54):18–31, 2012.

[8] Egil Fagerholt. *Field Measurements in Mechanical Testing Using Close-Range Photogrammetry and Digital Image Analysis*. PhD thesis, Norwegian University of Science and Technology, NTNU, 2012.

[9] Heine Røstum and Olve Winjum. Mechanical response of thermoplastics. Norwegian University of Science and Technology, NTNU, 2013.

[10] Torgrim Østen. Validation of material model for polyvinyl chloride (pvc). Master's thesis, Norwegian University of Science and Technology, NTNU, 2012.

Appendix A

LS-DYNA k-files

The simulations were run using a k-file called main.k. This file used the *INCLUDE command to include the material, mesh, load curve and contact conditions that were defined in separate files. The main.k example given here is for the simulation of PVC CC test number 1, but the files included can be changed depending on which test is run.

A.1 main.k

```
*KEYWORD
*INCLUDE
CC.k
PVC.k
curve-PVCCC-1.k
contact.k
*CONTROL_TIMESTEP
$#  dtinit    tssfac      isdo    tslimt     dt2ms      lctm     erode     ms1st
     0.000  0.900000         0     0.000     0.000         0         0         0
$#  dt2msf   dt2mslc     imscl
     0.000         0         0
*DATABASE_BNDOUT
$#      dt    binary      lcur     ioopt
  0.250000         1         0         1
*DATABASE_ELOUT
$#      dt    binary      lcur     ioopt
  0.250000         1         0         1
*DATABASE_NODFOR
$#      dt    binary      lcur     ioopt
  0.250000         1         0         1
*DATABASE_NODOUT
$#      dt    binary      lcur     ioopt      dthf     binhf
  0.250000         1         0         1     0.000         0
*DATABASE_BINARY_D3PLOT
$#      dt      lcdt      beam     npltc    psetid
  0.500000         0         0         0         0
$#   ioopt
         0
```

```
*DATABASE_EXTENT_BINARY
$#   neiph     neips    maxint    strflg    sigflg    epsflg    rltflg    engflg
         0         0         3         1         1         1         1         1
$#  cmpflg    ieverp    beamip     dcomp      shge     stssz    n3thdt   ialemat
         0         0         0         1         1         1         2         1
$# nintsld   pkp_sen      sclp    unused     msscl     therm    intout    nodout
         1         0  1.000000         0         0         0STRESS    STRESS
*DATABASE_NODAL_FORCE_GROUP
$#    nsid       cid
         1         0
*DATABASE_HISTORY_NODE_SET
$#     id1       id2       id3       id4       id5       id6       id7       id8
         6         7         0         0         0         0         0         0
*DATABASE_HISTORY_SOLID_SET
$#     id1       id2       id3       id4       id5       id6       id7       id8
         1         0         0         0         0         0         0         0
*BOUNDARY_PRESCRIBED_MOTION_RIGID
$#     pid       dof       vad      lcid        sf       vid     death     birth
         3         1         2         2  1.000000         01.0000E+28     0.000
*PART
$# title
HDPE
$#     pid     secid       mid     eosid      hgid      grav    adpopt      tmid
         1         1         1         0         0         0         0         0
*SECTION_SOLID
$#   secid    elform       aet
         1        -1         0
*END
```

A.2 Mesh files

The mesh files include node and element list, node and element sets and boundary conditions. The node and element lists are not included in the appendix.

A.2.1 TQ.k

```
*BOUNDARY_SPC_SET
$#    nsid       cid      dofx      dofy      dofz     dofrx     dofry     dofrz
         2         0         1         0         0         0         0         0
*SET_NODE_LIST_TITLE
bottom
$#     sid       da1       da2       da3       da4    solver
         2     0.000     0.000     0.000     0.000MECH
$#    nid1      nid2      nid3      nid4      nid5      nid6      nid7      nid8
```

```
      1730      1731      1732      1733      1734      1735      1736      1737
      1738      1739      1740      1741      1742      1743      1744      1745
      1746      1747      1748      1749      1750      1758      1763      1768
      1772      1782      1783      1789      1791      1793      1795      1798
      1801      1802      1810      1814      1815      1816      1817      1818
      1821      1822      1823      1824      1825      1826      1827      1831
      1832      1833      1834      1835      1837      1843      1845      1846
      1849      1851      1853      1867      1868      1873      1876         0
*BOUNDARY_SPC_SET
$#     nsid       cid      dofx      dofy      dofz     dofrx     dofry     dofrz
         3         0         0         0         0         0         1         1
*SET_NODE_LIST_TITLE
top
$#      sid       da1       da2       da3       da4    solver
         3     0.000     0.000     0.000     0.000MECH
$#     nid1      nid2      nid3      nid4      nid5      nid6      nid7      nid8
       568       569       570       571       572       573       574       575
       576       577       578       579       580       581       582       583
       584       585       586       587       588       596       601       606
       610       620       621       627       629       631       633       636
       639       640       648       652       653       654       655       656
       659       660       661       662       663       664       665       669
       670       671       672       673       675       681       683       684
       687       689       691       705       706       711       714         0
*BOUNDARY_SPC_SET
$#     nsid       cid      dofx      dofy      dofz     dofrx     dofry     dofrz
         4         0         0         1         0         1         0         1
*SET_NODE_LIST_TITLE
xz
$#      sid       da1       da2       da3       da4    solver
         4     0.000     0.000     0.000     0.000MECH
$#     nid1      nid2      nid3      nid4      nid5      nid6      nid7      nid8
         1         2         3         4         5         6         7         8
         9        10        11        12        13        14        15        16
        17        18        19        20        21        22        23        24
        25        26        27        28        29        30        31        32
        33        34        35        36        37        38        39        40
        41        42        43        44        45        46        47        48
        49        50        51        52        53        54        55        56
        57        58        59        60        61        62        63       446
       447       448       449       450       469       470       502       528
       539       552       557       563       564       589       590       603
       605       610       622       623       625       632       633       635
       637       641       643       647       649       650       651       662
       663       664       671       676       682       683       707       712
```

```
       713       820       822       823       828       833       834       835
       836       837       844       846       849       856       859       861
       865       866       873       874       877       879       880       886
       887       888       889       893       894       899       903       911
       914       946       947       948       949       950       951       952
       953       955       956       963       965       966       972       973
       976       981      1163      1164      1165      1166      1167      1168
      1169      1170      1171      1172      1173      1174      1175      1176
      1177      1178      1179      1180      1181      1182      1183      1184
      1185      1186      1187      1188      1189      1190      1191      1192
      1193      1194      1195      1196      1197      1198      1199      1200
      1201      1202      1203      1204      1205      1206      1207      1208
      1209      1210      1211      1212      1213      1214      1215      1216
      1217      1218      1608      1609      1610      1611      1612      1631
      1632      1664      1690      1701      1714      1719      1725      1726
      1751      1752      1765      1767      1772      1784      1785      1787
      1794      1795      1797      1799      1803      1805      1809      1811
      1812      1813      1824      1825      1826      1833      1838      1844
      1845      1869      1874      1875      1982      1984      1985      1990
      1995      1996      1997      1998      1999      2006      2008      2011
      2018      2021      2023      2027      2028      2035      2036      2039
      2041      2042      2048      2049      2050      2051      2055      2056
      2061      2065      2073      2076      2108      2109      2110      2111
      2112      2113      2114      2115      2117      2118      2125      2127
      2128      2134      2135      2138      2143         0         0         0
*BOUNDARY_SPC_SET
$#     nsid       cid      dofx      dofy      dofz     dofrx     dofry     dofrz
         5         0         0         0         1         1         1         0
*SET_NODE_LIST_TITLE
xy
$#      sid       da1       da2       da3       da4    solver
         5     0.000     0.000     0.000     0.000MECH
$#     nid1      nid2      nid3      nid4      nid5      nid6      nid7      nid8
         1         8        15        22        29        36        43        50
        57        64        71        78        85        92        99       106
       113       120       127       134       141       148       155       162
       169       176       183       190       197       204       211       218
       225       232       239       246       253       260       267       274
       281       288       295       302       309       316       323       330
       337       344       351       358       365       372       379       386
       393       400       407       414       421       428       435       443
       444       445       457       462       468       469       491       499
       511       521       522       526       529       539       546       550
       562       589       590       591       595       596       598       602
       607       611       614       615       618       621       630       638
```

```
       642       644       645       666       669       674       682       683
       684       687       689       690       691       694       695       696
       697       698       699       700       706       824       825       827
       835       849       854       860       863       871       872       878
       883       885       891       897       916       917       918       919
       920       921       922       923       924       925       931       934
       935       936       937       938       939       940       941       947
       948       949       950       951       958       959       968       969
       971       974       975       978       983       987      1163      1170
      1177      1184      1191      1198      1205      1212      1226      1233
      1240      1247      1254      1261      1268      1275      1289      1296
      1303      1310      1317      1324      1331      1338      1352      1359
      1366      1373      1380      1387      1394      1401      1415      1422
      1429      1436      1443      1450      1457      1464      1478      1485
      1492      1499      1506      1513      1520      1527      1541      1548
      1555      1562      1569      1576      1583      1590      1605      1606
      1607      1619      1624      1630      1631      1653      1661      1673
      1683      1684      1688      1691      1701      1708      1712      1724
      1751      1752      1753      1757      1758      1760      1764      1769
      1773      1776      1777      1780      1783      1792      1800      1804
      1806      1807      1828      1831      1836      1844      1845      1846
      1849      1851      1852      1853      1856      1857      1858      1859
      1860      1861      1862      1868      1986      1987      1989      1997
      2011      2016      2022      2025      2033      2034      2040      2045
      2047      2053      2059      2078      2079      2080      2081      2082
      2083      2084      2085      2086      2087      2093      2096      2097
      2098      2099      2100      2101      2102      2103      2109      2110
      2111      2112      2113      2120      2121      2130      2131      2133
      2136      2137      2140      2145      2149         0         0         0
*SET_NODE_LIST_TITLE
center
$#     sid       da1       da2       da3       da4    solver
         1     0.000     0.000     0.000     0.000MECH
$#    nid1      nid2      nid3      nid4      nid5      nid6      nid7      nid8
        57        58        59        60        61        62        63       120
       121       122       123       124       125       126       183       184
       185       186       187       188       189       246       247       248
       249       250       251       252       309       310       311       312
       313       314       315       372       373       374       375       376
       377       378       435       436       437       438       439       440
       441         0         0         0         0         0         0         0
*SET_NODE_LIST_TITLE
disp
$#     sid       da1       da2       da3       da4    solver
         6     0.000     0.000     0.000     0.000MECH
```

```
$#    nid1      nid2      nid3      nid4      nid5      nid6      nid7      nid8
       568         0         0         0         0         0         0         0
*SET_NODE_LIST_TITLE
strains
$#     sid       da1       da2       da3       da4    solver
         7     0.000     0.000     0.000     0.000MECH
$#    nid1      nid2      nid3      nid4      nid5      nid6      nid7      nid8
        56        63       119       126       182       189       245       252
       308       315       371       378       434       441         0         0
*SET_SOLID_TITLE
section
$#     sid    solver
         1MECH
$#      k1        k2        k3        k4        k5        k6        k7        k8
        43        44        45        46        47        48        91        92
        93        94        95        96       139       140       141       142
       143       144       187       188       189       190       191       192
       235       236       237       238       239       240       283       284
       285       286       287       288         0         0         0         0
```

A.2.2 TC.k

```
*TITLE
$# title
LS-DYNA keyword deck by LS-PrePost
*BOUNDARY_SPC_SET
$#    nsid       cid      dofx      dofy      dofz     dofrx     dofry     dofrz
         2         0         1         0         0         0         0         0
*SET_NODE_LIST_TITLE
bottom
$#     sid       da1       da2       da3       da4    solver
         2     0.000     0.000     0.000     0.000MECH
$#    nid1      nid2      nid3      nid4      nid5      nid6      nid7      nid8
       998       999      1000      1002      1004      1009      1022      1023
      1028      1030      1031      1032      1034      1055      1056      1057
      1058      1059      1060      1061      1062      1063      1064      1065
      1066      1067      1068      1069      1070      1071      1072      1073
      1074      1075      1076      1077      1099      1100      1103      1108
      1109      1110      1111         0         0         0         0         0
*BOUNDARY_SPC_SET
$#    nsid       cid      dofx      dofy      dofz     dofrx     dofry     dofrz
         3         0         0         0         0         0         1         1
*SET_NODE_LIST_TITLE
top
$#     sid       da1       da2       da3       da4    solver
```

```
         3     0.000     0.000     0.000     0.000MECH
$#    nid1      nid2      nid3      nid4      nid5      nid6      nid7      nid8
        52        53        54        56        58        63        76        77
        82        84        85        86        88       109       110       111
       112       113       114       115       116       117       118       119
       120       121       122       123       124       125       126       127
       128       129       130       131       153       154       157       162
       163       164       165         0         0         0         0         0
*BOUNDARY_SPC_SET
$#    nsid       cid      dofx      dofy      dofz     dofrx     dofry     dofrz
         4         0         0         1         0         1         0         1
*SET_NODE_LIST_TITLE
xz
$#     sid       da1       da2       da3       da4    solver
         4     0.000     0.000     0.000     0.000MECH
$#    nid1      nid2      nid3      nid4      nid5      nid6      nid7      nid8
        24        25        30        32        33        34        39        44
        46        47        52        53        54        58        59        61
        62        63        65        66        74        79        82        83
        89        90        95        98        99       100       101       102
       103       104       105       106       107       108       155       157
       159       166       259       260       261       262       263       264
       265       266       267       268       269       270       271       272
       273       274       275       276       277       278       279       280
       281       282       283       284       285       393       395       397
       400       401       402       403       416       417       418       419
       422       426       427       428       429       433       435       436
       437       441       442       444       446       448       449       450
       453       477       478       479       480       481       482       483
       484       682       686       695       696       697       698       699
       701       702       703       704       705       706       707       708
       709       710       711       712       713       714       717       718
       719       720       721       722       723       724       725       726
       727       728       729       730       764       765       766       767
       768       769       770       771       772       773       774       775
       776       777       970       971       976       978       979       980
       985       990       992       993       998       999      1000      1004
      1005      1007      1008      1009      1011      1012      1020      1025
      1028      1029      1035      1036      1041      1044      1045      1046
      1047      1048      1049      1050      1051      1052      1053      1054
      1101      1103      1105      1112      1205      1206      1207      1208
      1209      1210      1211      1212      1213      1214      1215      1216
      1217      1218      1219      1220      1221      1222      1223      1224
      1225      1226      1227      1228      1229      1230      1231      1339
      1341      1343       400       401       402       403      1362      1363
```

```
      1364      1365      1368      1372      1373      1374      1375      1379
      1381       436       437      1387      1388       444      1392      1394
      1395      1396      1399      1423      1424      1425      1426      1427
      1428      1429      1430      1628      1632      1641      1642      1643
      1644      1645      1647      1648      1649      1650      1651      1652
      1653      1654      1655      1656      1657      1658      1659      1660
      1663      1664      1665      1666      1667      1668      1669      1670
      1671      1672      1673      1674      1675      1676      1710      1711
      1712      1713      1714      1715      1716      1717      1718      1719
      1720      1721      1722      1723         0         0         0         0
*BOUNDARY_SPC_SET
$#     nsid       cid      dofx      dofy      dofz     dofrx     dofry     dofrz
         5         0         0         0         1         1         1         0
*SET_NODE_LIST_TITLE
xy
$#      sid       da1       da2       da3       da4    solver
         5     0.000     0.000     0.000     0.000MECH
$#     nid1      nid2      nid3      nid4      nid5      nid6      nid7      nid8
        24        27        31        35        36        37        43        45
        49        50        56        59        61        80        82        89
       132       133       134       135       136       137       138       139
       140       141       142       143       144       145       146       147
       148       149       150       151       153       162       163       164
       165       166       335       336       337       338       339       340
       341       342       343       344       345       346       347       348
       349       350       351       352       353       354       355       356
       357       358       359       360       361       362       363       364
       365       366       367       368       369       395       396       398
       399       411       412       413       414       415       416       417
       418       421       422       424       425       426       430       432
       434       436       438       439       442       443       445       448
       452       646       647       648       649       650       651       652
       653       654       655       656       657       658       659       660
       661       662       663       664       665       666       667       668
       669       670       671       672       724       725       726       727
       728       729       730       731       732       733       734       735
       736       737       778       779       780       781       782       783
       784       785       970       973       977       981       982       983
       989       991       995       996      1002      1005      1007      1026
      1028      1035      1078      1079      1080      1081      1082      1083
      1084      1085      1086      1087      1088      1089      1090      1091
      1092      1093      1094      1095      1096      1097      1099      1108
      1109      1110      1111      1112      1281      1282      1283      1284
      1285      1286      1287      1288      1289      1290      1291      1292
      1293      1294      1295      1296      1297      1298      1299      1300
```

```
      1301      1302      1303      1304      1305      1306      1307      1308
      1309      1310      1311      1312      1313      1314      1315      1341
      1342      1344      1345       411       412       413       414       415
      1362      1363      1364       421      1368      1370      1371      1372
      1376      1378      1380       436      1384      1385      1388      1389
      1391      1394      1398      1592      1593      1594      1595      1596
      1597      1598      1599      1600      1601      1602      1603      1604
      1605      1606      1607      1608      1609      1610      1611      1612
      1613      1614      1615      1616      1617      1618      1670      1671
      1672      1673      1674      1675      1676      1677      1678      1679
      1680      1681      1682      1683      1724      1725      1726      1727
      1728      1729      1730      1731         0         0         0         0
*SET_NODE_LIST_TITLE
center
$#     sid       da1       da2       da3       da4    solver
         1     0.000     0.000     0.000     0.000MECH
$#    nid1      nid2      nid3      nid4      nid5      nid6      nid7      nid8
       370       371       372       373       374       375       376       377
       378       379       380       381       382       383       384       385
       386       387       388       389       390       391       392       400
       401       402       403       404       405       406       407       408
       409       410       411       412       413       414       415       421
       436       437       444       370       371       372       373       374
       375       376       377       378       379       380       381       382
       383       384       385       386       387       388       389       390
       391       392       400       401       402       403       404       405
       406       407       408       409       410       411       412       413
       414       415       421       436       437       444         0         0
*SET_NODE_LIST_TITLE
disp
$#     sid       da1       da2       da3       da4    solver
         6     0.000     0.000     0.000     0.000MECH
$#    nid1      nid2      nid3      nid4      nid5      nid6      nid7      nid8
        52         0         0         0         0         0         0         0
*SET_NODE_LIST_TITLE
strains
$#     sid       da1       da2       da3       da4    solver
         7     0.000     0.000     0.000     0.000MECH
$#    nid1      nid2      nid3      nid4      nid5      nid6      nid7      nid8
       419       437       404       316       319       405       406       322
       325       407       408       334       331       409       410       328
       443       421         0         0         0         0         0         0
*SET_SOLID_TITLE
section
$#     sid    solver
```

```
         1MECH
$#      k1          k2          k3          k4          k5          k6          k7          k8
       292         296         300         304         308         312         316         320
       321         322         323         324         337         338         339         340
       353         354         355         356         369         370         371         372
       388         392         396         400         404         408         412         416
```

A.3 Material files

A.3.1 HDPE.k

```
*MAT_USER_DEFINED_MATERIAL_MODELS
$#     mid         ro          mt         lmc         nhv      iortho      ibulk         ig
         1  9.400000          46          16          50           0          15          16
$#   ivect      ifail     itherm     ihyper       ieos       lmca     unused     unused
         1          0          0          1          0          0          0          0
$        E         PR       Eps0         Ct         St         Cr        Lam      Alpha
      1400       0.43   1.00E-02       0.12       12.1        1.5        5.6       1.00
$     beta                 Sigsat          H    Epsfail                   K          G
      1.07        0.0       26.10      56.00                             3333        490
*END
```

A.3.2 PVC.k

```
*MAT_USER_DEFINED_MATERIAL_MODELS
$#     mid         ro          mt         lmc         nhv      iortho      ibulk         ig
         1 940.00E-2          46          16          50           0          15          16
$#   ivect      ifail     itherm     ihyper       ieos       lmca     unused     unused
         1          0          0          1          0          0          0          0
$        E         PR       Eps0         Ct         St         Cr        Lam      Alpha
      2800       0.38   1.00E-03       0.07       44.4       10.2       2.28       1.33
$     beta                 Sigsat          H    Epsfail                   K          G
      1.16        0.0       31.20      12.00                             3889       1015
```

A.4 Displacement curve

The displacement curves were created using the displacement history of the experimental tests. The example given here is from the cyclic test HDPE TQ 6.

```
*CONTROL_TERMINATION
$#  endtim    endcyc     dtmin    endeng    endmas
 4854.0000         0    0.0000    0.0000    0.0000
*DEFINE_CURVE
```

```
$#    lcid      sidr       sfa       sfo      offa      offo    dattyp
         2         0  1.000000  1.000000     0.000     0.000         0
$#              a1                  o1
           0.000000            0.000000
         206.000000            2.591300
         314.000000            1.247615
         530.000000            3.993521
         630.000000            2.760988
         864.000000            5.744325
         978.000000            4.319742
        1308.000000            8.542849
        1448.000000            6.782837
        3466.000000           32.942337
        3780.000000           28.916528
        4864.000000           42.833568
```

A.5 Contact conditions

This k-file is only used for the compression tests. It defines the material properties of the two boxes used in the simulation, and the conditions of the contact surface.

```
*CONTACT_AUTOMATIC_SINGLE_SURFACE_ID
$#     cid                                                          title
         1
$#    ssid      msid     sstyp     mstyp    sboxid    mboxid       spr       mpr
         1         0         2         0         0         0         0         0
$#      fs        fd        dc        vc       vdc    penchk        bt        dt
  0.060000  0.000000     0.000     0.000     0.000         0     0.0001.0000E+20
$#     sfs       sfm       sst       mst      sfst      sfmt       fsf       vsf
 10.000000  1.000000     0.000     0.000  1.000000  1.000000  1.000000  1.000000
*PART
$# title
top
$#     pid     secid       mid     eosid      hgid      grav    adpopt      tmid
         3         1         3         0         0         0         0         0
*MAT_RIGID_TITLE
top
$#     mid        ro         e        pr         n    couple         m     alias
        35.0000E-10 1.000E+04  0.300000     0.000     0.000     0.000
$#     cmo      con1      con2
  1.000000         5         7
$# lco or a1      a2        a3        v1        v2        v3
     0.000     0.000     0.000     0.000     0.000     0.000
*PART
```

```
$# title
bottom
$#     pid     secid       mid     eosid      hgid      grav    adpopt      tmid
         4         1         4         0         0         0         0         0
*MAT_RIGID_TITLE
bottom
$#     mid        ro         e        pr         n    couple         m     alias
        45.0000E-10 1.000E+04  0.300000     0.000     0.000     0.000
$#     cmo      con1      con2
  1.000000         7         7
$# lco or a1      a2        a3        v1        v2        v3
     0.000     0.000     0.000     0.000     0.000     0.000
*SET_PART_LIST_TITLE
Slave
$#     sid       da1       da2       da3       da4    solver
         1     0.000     0.000     0.000     0.000MECH
$#    pid1      pid2      pid3      pid4      pid5      pid6      pid7      pid8
         1         3         4         0         0         0         0         0
*SET_PART_LIST_TITLE
Master
$#     sid       da1       da2       da3       da4    solver
         2     0.000     0.000     0.000     0.000MECH
$#    pid1      pid2      pid3      pid4      pid5      pid6      pid7      pid8
         3         4         0         0         0         0         0         0
```

Appendix B

Matlab scripts

Here, the Matlab scripts used for obtaining the results of the experimental tests and simulations are presented.

B.1 testdata.m

This script reads the file written by the test machine containing the force and displacement of the experimental tests. It also reads the file written by eCorr that contains the strains of the tests.

```
clear all
clc

mat = 'HDPE';
geo = 'RUTS6';

for test = 1:2

dir = ['C:\Master\' mat '\' geo '\'];

% Load log file
fLog = [geo '-' num2str(test) '_Log.txt'];
A = importdata([dir fLog],'\t',5); A = A.data;
col = size(A,2);
if col == 5
    A(:,3) = [];
end

[removed,sm,steps,slutt] = testedit(mat,geo,test,A);
A(slutt:end,:) = [];

% Extract frame, time, force and displacement
fr = A(:,1);
t = A(:,2);
F = A(:,3);
D = A(:,4);
```

```
if strncmp(mat,'HDPE',4) && strncmp(geo,'RUT66',5) && test <= 4
    testdata2D;
else
    % Load strains and sides
    feps = ['strains\' geo '-' num2str(test) '_strains.txt'];

    % Extract strains
    eps = importdata([dir feps],',',4); eps = eps.data;
    [row,col] = size(eps);
    Nele = col/2;
    if strncmp(geo,'Trykk',5)
        epsTe = eps(:,1:Nele);
        epsLe = eps(:,Nele+1:col);
    else
        epsLe = eps(:,1:Nele);
        epsTe = eps(:,Nele+1:col);
    end
end
epsLe(slutt:end,:) = [];
epsTe(slutt:end,:) = [];

% Strain rate
Depse = zeros(size(epsLe));
for j = 1:size(epsLe,2)
    for i = 2:size(epsLe,1)-1
        Depse(i,j) = (epsLe(i+1,j)-epsLe(i-1,j))/(t(i+1)-t(i-1));
    end
end

% Area and volumetric strain, and mean strains
if strncmp(geo,'RUT66',5)
    epsAe = 2*epsTe;
else
    epsAe = log(exp(epsTe).^2);
end
epsVe = epsLe + epsAe;

epsL = mean(epsLe,2);
epsT = mean(epsTe,2);
epsA = mean(epsAe,2);
epsV = mean(epsVe,2);
```

```
Deps = mean(Depse,2);

% Formatting data to start at zero
D(1:removed) = [];
F(1:removed) = [];
epsL(1:removed) = [];
epsT(1:removed) = [];
epsA(1:removed) = [];
epsV(1:removed) = [];
Deps(1:removed) = [];

if ~strcmp(mat,'PVC') || ~strcmp(geo,'RUT66') || test ~= 5
    D = D - D(1);
    F = F - F(1);
    epsL = epsL - epsL(1);
    epsT = epsT - epsT(1);
    epsA = epsA - epsA(1);
    epsV = epsV - epsV(1);
    Deps = Deps - Deps(1);
end

D = [zeros(removed,1); D];
F = [zeros(removed,1); F];
epsL = [zeros(removed,1); epsL];
epsT = [zeros(removed,1); epsT];
epsA = [zeros(removed,1); epsA];
epsV = [zeros(removed,1); epsV];
Deps = [zeros(removed,1); Deps];

for i = 1:sm
    D(1:steps) = smooth(D(1:steps));
    D(1) = 0;
    F(1:steps) = smooth(F(1:steps));
    F(1) = 0;
    epsL(1:steps) = smooth(epsL(1:steps));
    epsL(1,:) = 0;
    epsT(1:steps) = smooth(epsT(1:steps));
    epsT(1,:) = 0;
    epsA(1:steps) = smooth(epsA(1:steps));
    epsA(1,:) = 0;
    epsV(1:steps) = smooth(epsV(1:steps));
    epsV(1,:) = 0;
```

```
    Deps(1:steps) = smooth(Deps(1:steps));
    Deps(1,:) = 0;
end

% Cross section area
if strcmp(geo,'RUT66')
    d0 = 6;
    d = d0*exp(epsT);
    A = d.^2;
elseif strcmp(geo,'RUTS6')
    r0 = 3;
    r = r0*exp(epsT);
    A = pi*r.^2;
elseif strcmp(geo,'Trykk')
    r0 = 4;
    r = r0*exp(epsT);
    A = pi*r.^2;
end

H = 10 + D;
if strcmp(geo,'Trykk')
    epssecL = log(H/H(1));
    epssecV = epssecL + epsA;
    Depssec = zeros(size(epssecL));
    for i = 2:length(epssecL)-1
        Depssec(i) = (epssecL(i+1)-epssecL(i-1))/(t(i+1)-t(i-1));
    end
end

% Stress
sig = 1000*F./A;
sig = sig - sig(1);

fclose all;

end
```

B.2 nodoutread.m

This script reads the nodout file from LS-DYNA, containing the displacement of the nodes of the numerical simulations. It also reads the bndout file, which contains the

force history of the simulations.

```
clear all
clc

mat = 'HDPE';
geo = 'Trykk';
test = 'nofric';

dir = ['C:\Master\LS-DYNA\' mat '\' geo '\' test];
nod = fopen([dir '\nodout']);

% Finding number of nodes
tline = fgetl(nod);
while ~strncmp(tline,' nodal',5)
    tline = fgetl(nod);
end
Nnod = 0;
while ~strcmp(tline,'')
    Nnod = Nnod + 1;
    tline = fgetl(nod);
end
fclose all;
Nnod = Nnod - 2;

% Extracting time, displacement and coordinates
nod = fopen([dir '\nodout']);
D = [0; 0];
F = D;
t = D;
k = 0;
s = 0;
while k < 20
    k = k + 1;
    tline = fgetl(nod);
    if strncmp(tline,' n o d',6) == 1
        s = s + 1;
        t(s) = sscanf(tline,'%*104c%f',[1 1]);
        fgetl(nod);
        fgetl(nod);

        if ~strcmp(geo,'RUT66')
            tline = str2num(fgetl(nod));
```

```
            D(s) = tline(2);
        end

        for i = 1:Nnod
            tline = str2num(fgetl(nod));
            C(i,:,s) = [tline(11:13) tline(1) 0];
        end

        if strcmp(geo,'RUT66')
            tline = str2num(fgetl(nod));
            D(s) = tline(2);
        end

        k = 0;
    end
end

% Sorting coordinate matrix
C(:,:,1) = sortrows(C(:,:,1),[2 1]);
for i = 1:Nnod
    nodnum(i,1) = i;
    if i < Nnod && abs(C(i,2,1) - C(i+1,2,1)) < 0.01;
        C(i,2,1) = C(i+1,2,1);
    end
end
C(:,:,1) = sortrows(C(:,:,1),[2 1]);
nodnum(:,2) = C(:,4,1);
for i = 1:s
    for j = 1:Nnod
        for k = 1:size(nodnum,1)
            if C(j,4,i) == nodnum(k,2)
                C(j,5,i) = nodnum(k,1);
            end
        end
    end
end
for i = 1:s
    C(:,:,i) = sortrows(C(:,:,i),5);
end

% Converting coordinates to strains
[epsLe,epsTe] = coord2strains(C,Nnod,s);
```

```
Depse = zeros(size(epsLe));
for j = 1:size(epsLe,2)
    for i = 2:size(epsLe,1)-1
        Depse(i,j) = (epsLe(i+1,j)-epsLe(i-1,j))/(t(i+1)-t(i-1));
    end
end

% Area and volumetric strains
if strncmp(geo,'RUT66',5)
    epsAe = 2*epsTe;
else
    epsAe = log(exp(epsTe).^2);
end
epsVe = epsLe + epsAe;

epsL = mean(epsLe,2);
epsT = mean(epsTe,2);
epsA = mean(epsAe,2);
epsV = mean(epsVe,2);
Deps = mean(Depse,2);

% Radius and area
if strcmp(geo,'RUT66')
    d0 = 6;
    d = d0*exp(epsT);
    A = d.^2;
else
    r0 = pytagoras([0 0 0],C(Nnod-1,1:3,1));
    r = r0*exp(epsTe(:,1));
    A = pi*r.^2;
end


fclose all;

bnd = fopen([dir '\bndout']);

k = 0;
s = 0;
while k < 400
    k = k + 1;
```

```
    tline = fgetl(bnd);
    if strncmp(tline,'              xtotal=',21) == 1
        s = s + 1;
        b = sscanf(tline,'%*22c%f',[1 1]);
        F(s) = 4*b/1000;
        k = 0;
    end
end

rev = reversal(mat,geo,test);
stop = 0;
if rev ~= 0
    for j = 1:length(rev)
        start = stop + 1;
        stop = rev(j) - 1;
        for k = 1:30
            F(start:stop) = smooth(F(start:stop));
            F(1) = 0;
        end
        F(rev(j)) = F(rev(j)-1);
    end
    F(end) = [];
else
    for j = 1:30
        F = smooth(F);
        F(1) = 0;
    end
end

sig = 1000*F./A;

fclose all;
```

B.3 eloutread.m

This script reads the elout file from LS-DYNA, containing the strains and stresses of the elements of the numerical simulations.

```
dir = ['C:\Master\LS-DYNA\' mat '\' geo '\' test];
el = fopen([dir '\elout']);

[Nele,center,corner,side] = sectionoutput(geo,test);
```

```
Nsid = length(side);

k = 0;
i = 0;
while k < 50
    k = k + 1;
    tline = fgetl(el);
    if strncmp(tline,' e l e m e n t   s t r e s s',28) == 1
        i = i + 1;

        % Time
        t(i) = sscanf(tline,'%*82c%*f%*12c%f',[1 1]);

        % Empty lines
        for j = 1:4
            fgetl(el);
        end

        for j = 1:Nele
            fgetl(el);
            tline = str2num(fgetl(el));

            s11e(i,j) = tline(2);
            s22e(i,j) = tline(3);
            s33e(i,j) = tline(4);
            s12e(i,j) = tline(5);
            s23e(i,j) = tline(6);
            s31e(i,j) = tline(7);
        end

        % Empty lines
        for j = 1:7
            fgetl(el);
        end

        for j = 1:Nele
            fgetl(el);
            tline = str2num(fgetl(el));

            % Strains section
            epssecLe(i,j) = tline(2);
            epssecTye(i,j) = tline(3);
```

```
            epssecTze(i,j) = tline(4);
        end

        k = 0;
    end
end

epssecAe = epssecTye + epssecTze;
epssecVe = epssecLe + epssecAe;

epssecL = mean(epssecLe,2);
epssecTy = mean(epssecTye,2);
epssecTz = mean(epssecTze,2);
epssecA = mean(epssecAe,2);
epssecV = mean(epssecVe,2);

sigsece = s11e;
sigsec = mean(sigsece,2);
Fs = sigsec.*A/1000;

fclose all;
```